Advances in Condensation Heat Transfer

ICHIRO TANASAWA

Institute of Industrial Science
University of Tokyo
Roppongi, Minato-ku, Tokyo 106, Japan

I. Introductory Remarks

Condensation is still one of the most important heat transfer processes in many energy conversion systems, such as electric power generation plants. As is well known, the industrial revolution in the eighteenth century owed much to improvements of steam engines by James Watt and other engineers; the greatest achievement that James Watt performed was that he greatly improved the efficiency of the steam condenser, which was a direct-contact type. Although the surface condenser, for which James Watt had taken a patent in 1769 [1], was not in practical use during Watt's lifetime, because of immature manufacturing technology, it has subsequently played a most significant role as a heat-removing device in power generation, refrigeration, or air conditioning systems.

The *theory* of heat transfer by condensation appeared much later than the development of condensers. Nusselt's pioneering paper [2] on film condensation of steam was published in 1916, a century and a half after Watt's work. A study on dropwise condensation by Schmidt *et al.* [3] was reported in 1930. Like most of the research in heat transfer, theories followed industrial developments.

However, the situation seems to be changing. Although steam and other vapors of pure substances have been employed as working fluids of the energy conversion cycles, use of multicomponent media is developing, especially in high-performance heat pump systems. Because condensation of multicomponent vapors is much more complex in nature, fundamental studies are indispensable before designing an industrial system, both from thermodynamical and from heat transfer points of view. Cooperation between fundamental research and design engineering becomes more important.

In this review an attempt has been made to put more emphasis on the areas of condensation heat transfer that have made progress in the past 15 years. Some of the fundamentals of condensation, such as nucleation and growth of a liquid droplet in bulk or surface condensation, are omitted. Basic mechanisms of dropwise condensation and direct contact condensation are not mentioned in detail. These are described in detail in other volumes of *Advances in Heat Transfer*. For example, homogeneous nucleation has been described by Springer [4], some of the mechanisms of dropwise condensation have been described by Merte [5], and direct contact condensation has been extensively discussed by Sideman and Moalem Maron [6].

In the present work, the various types of condensation are introduced in Section II. Then the wettability of the surface, which determines the mode of surface condensation, film or dropwise, is discussed.

In Section III the transport process at the vapor–liquid interface and the arguments on whether the condensation coefficient takes the value of unity are discussed. In Section IV dropwise condensation is dealt with, focusing attention on the results of recent investigations. Also described are how to promote dropwise condensation and how to maintain it in condensers for industrial use.

Film condensation is discussed in Section V. However, the classical theory of film condensation is skipped, and only the results of recent achievements are introduced. Special emphasis is put on condensation of multicomponent vapors. Use of multicomponent working fluids has become more important to increase efficiencies of thermodynamic cycles for advanced heat pump systems. However, there remains much to be done to predict and enhance heat transfer performance of condensers in which multicomponent vapors condense.

Section VI is assigned to the techniques of enhancement of condensation heat transfer. In principle, there are not so many choices for the augmentation of condensation. Use of surface tension force is one of the most sophisticated ways for it, because it does not require extra energy. However, it has been confirmed lately that an electric field is very efficient for this purpose, although the method requires the consumption of some electric power. Examples of both of the techniques are discussed in some detail. Concluding remarks include the author's personal view on the future trends in research on condensation heat transfer.

More than 100 publications are provided as references. However, this is not a complete list of publications on condensation heat transfer. On the contrary, a considerable number of excellent papers are not cited. Works done by our predecessors and colleagues are selectively quoted only whenever it proved necessary. When similar papers had been published on a certain subject, sometimes only one of them was quoted, although an attempt was made to

choose the paper published earlier. The author would hope that this writing will make some contribution to the further development of condensation heat transfer.

II. Fundamentals of Condensation

A. TYPES OF CONDENSATION

In this work the word "condensation" represents the change of phase from the vapor state to the liquid state due to cooling. When the vapor is cooled strongly enough, the liquid phase changes further to the solid phase. Or, in some cases, the vapor, when cooled, turns directly into a solid. This last process is the reverse process of sublimation. Condensation that proceeds to solidification is out of the scope of this text.

From the microscopic point of view, condensation takes place when the molecules in the vapor phase impinge on the liquid surface, which is in contact with the vapor, and remain there in the liquid. However, there are always some molecules escaping from the liquid surface into the vapor, freed from the intermolecular force field acting in the liquid phase. This is microscopic description of the evaporation process. Net condensation occurs when the number of molecules crossing a unit area of the vapor–liquid interface per unit time into the liquid phase is larger than the number crossing toward the vapor phase. When the number of impinging molecules exceeds the number of escaping molecules, net evaporation is said to occur. Usually the adjective "net" is omitted and net condensation and net evaporation are simply called condensation and evaporation. The microscopic process of condensation will be discussed in more detail in another section of this article.

As mentioned, condensation is the reverse process of evaporation. However, condensation is often discussed in contrast to boiling. It is not always exact because boiling is merely a type of evaporation in which the liquid vaporizes into the vapor phase formed in the bulk of the liquid.

Condensation is classified into homogeneous condensation and heterogeneous condensation. The former occurs in a space where no foreign substance exists. It takes place stochastically as the result of fluctuation of motion of the vapor molecules. Such a process rarely plays an important role in actual heat-transferring devices. On the other hand, the latter occurs with the aid of foreign materials, liquid or solid, forming the liquid phase on its surface or by using it as a nucleus.

Heterogeneous condensation is divided further into condensation in space (volume or bulk condensation) and condensation on a surface (surface

condensation). Volume condensation takes place by making use of the small particles of liquid or solid, which are floating in space, as the nuclei. An example is the formation of clouds, mist, or fog. Apart from its phenomenological interest, volume condensation was rarely considered to be important so far as industrial applications were concerned. However, deposition of sodium vapor on a solid wall occurring in the liquid-metal-cooled fast-breeder nuclear reactor, which is now being developed, offers a problem of practical importance. The process is as follows. Liquid sodium, used as the primary coolant in the fast-breeder reactor (FBR) core, evaporates into argon, which is used as the cover gas. Then it is carried upward to a rotating plug or to the other solid walls by diffusion and/or convection and is deposited there. If the deposited sodium is solidified, it causes an operational problem. Recent investigation of this phenomenon has revealed that the rate of evaporation and, consequently, the rate of deposition of sodium increase to a great extent by formation of sodium mist in the bulk of argon gas. The higher the rate of volume condensation, the larger the probability of occurrence of trouble. Although similar phenomena are observed in devices such as refrigerators operated in low temperatures, fewer studies have been made on volume condensation than on surface condensation.

Surface condensation is subdivided into condensation onto liquid surfaces and condensation onto solid surfaces. The former includes direct contact condensation on drops, jets, or films of liquid and the process of collapse of the vapor bubble during subcooled boiling. The number of practical applications is considerable. Solid surface condensation is literally condensation on a solid wall kept at low temperature. However, if we observe this process more closely, the vapor phase is not always in touch directly with the solid wall, because a layer of liquid is usually formed on it. Nevertheless, this type of surface condensation is different from vapor–liquid direct-contact condensation in the sense that the solid wall plays an important role in transfer of heat.

When we notice the form of the liquid phase on the solid surface, we can distinguish dropwise condensation from film condensation. These two typical types of condensation will be discussed in the following section.

The classification of condensation as mentioned above is illustrated in Fig. 1. Speaking very roughly, most of the research in heat transfer by condensation up to the present has been performed with regard to heterogeneous, surface, solid surface, and film condensation (categories B, b, β, and ii in Fig. 1). However, the recent tendency seems to indicate an interest in homogeneous, liquid surface, and dropwise condensation (a, α, and i) as the new areas of research. A more detailed discussion is not provided here, because it is not the objective of this article.

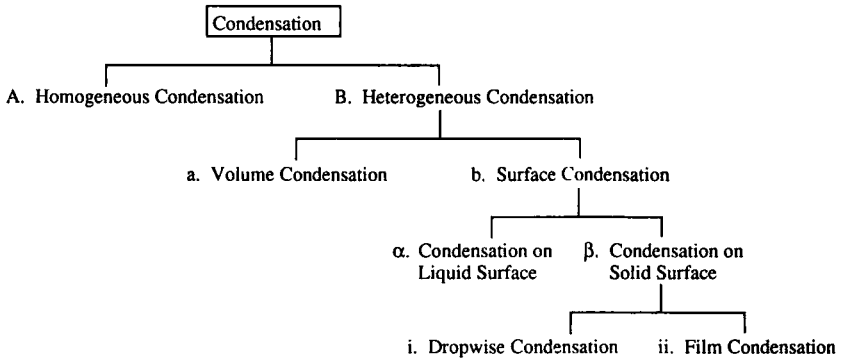

FIG. 1. Classification of condensation phenomena.

B. FILM CONDENSATION AND DROPWISE CONDENSATION

When condensation takes place on a solid surface, it occurs in one of two ways: dropwise or film condensation. Which of these two processes occurs is determined by the wettability of the solid surface.

If the liquid formed by condensation does wet the surface, film condensation is observed. In film condensation, the liquid condensate forms a continuous film over the surface. This film flows down the surface under the actions of gravity, shear force due to vapor flow, or other forces. The latent heat released at the vapor–liquid interface is transferred through the condensate film and then through the solid wall, and is finally removed by a coolant, which in many cases is flowing on the other side of the condensing surface. A steady state is established when the rate of condensation is balanced with the rate of flow of the condensate. As is obvious from the above description, the rate of heat transfer by film condensation is determined by the thickness of the condensate film, which forms, in most cases, the greatest portion of the thermal resistance. The situation is different in the case of dropwise condensation. Shown in Fig. 2 are sketches of film and dropwise condensation processes and a picture of dropwise condensation.

Dropwise condensation takes place when the liquid condensate does not wet the solid surface. The condensate does not spread, but forms separate drops. The process of dropwise condensation consists of a combination of several random processes. It is more easily understood if we view it as a cycle composed of four elemental subprocesses as shown in Fig. 3.

After the vapor impinges on a surface cooled to a temperature below the saturation temperature, numerous minute droplets (initial droplets) are

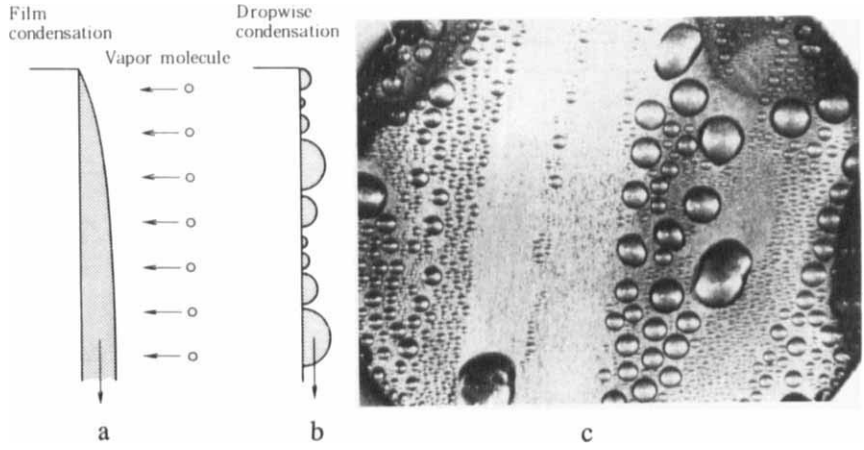

FIG. 2. Film and dropwise condensation.

formed, releasing the latent heat of condensation. These droplets grow very rapidly due to the continuing direct condensation of vapor onto them. Because the distances between neighboring droplets are very small, some of the droplets touch each other and coalesce to form larger drops by the action of surface tension force. At each coalescence, the drops shift their positions a little, leaving open areas on the surface where initial droplets are generated again. These droplets also grow by direct condensation and coalescence, but

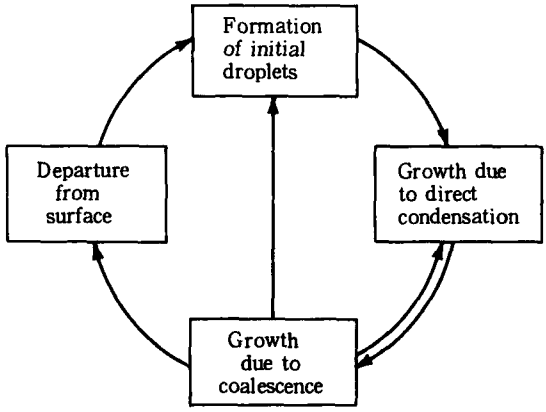

FIG. 3. Cycle of dropwise condensation.

most of them vanish when they are absorbed by larger neighboring drops. Because the process of drop growth is the repetition of two steps, frequent condensation and coalescence as described above, it is almost impossible and does not make sense to attempt to treat these two steps separately. There have been a number of studies in which such a mistake has been made in discussing the process of drop growth. At any rate, when the drops grow to a certain limiting size, which we call "departure size," they are swept off the surface by the actions of gravity, vapor shear force, and other external forces. As the drops depart the surface, they take in other droplets within their path, sweeping clean a portion of the surface, where again droplets generate anew. Thus, one cycle of dropwise condensation is completed.

To fully understand these four fundamental subprocesses, which comprise the entire cycle of dropwise condensation, and to know the interrelation between these subprocesses as well, are the essential tasks in investigating the mechanism of dropwise condensation. As will be discussed in Section IV, such tasks await further elucidation.

C. WETTABILITY

When vapor condenses on a cooled surface, the type of condensation, film or dropwise, that does occur is dependent upon whether the liquid condensate wets the surface. In the present case, the word "wet" means a phenomenon illustrated in Fig. 4. When we place a drop of liquid on a solid surface, either the drop spreads over the surface to form a thin film or it does not spread, but rather forms a cap-shaped droplet. In the former case we say the liquid wets the surface, and in the latter case we say the liquid does not wet the surface. As everyone may understand at once, this phenomenon is related to the surface tension of the liquid. However, things are not so simple. If, then, we try to put a small amount of liquid into a capillary tube, as illustrated in Fig. 5, the liquid either proceeds into the tube or it will not go

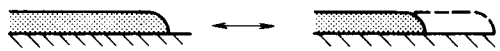

FIG. 4. Wettability of a solid surface.

FIG. 5. Wettability in a capillary tube.

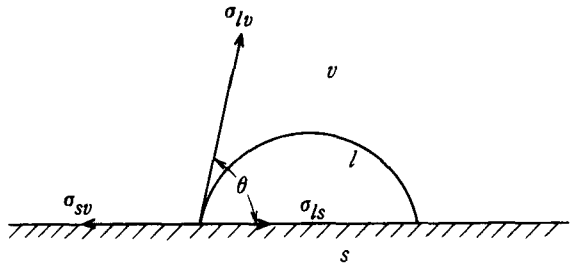

FIG. 6. Balance between interfacial forces.

into the tube. We may say that the liquid wet the tube in the former case, but that it does not wet the tube in the latter case. The criterion of wettability in this situation is different from that of the case shown in Fig. 4. Let us now discuss the situation drawn in Fig. 4.

When a pure vapor condenses on a solid surface, three phases appear: solid, liquid, and vapor. Three kinds of interfaces exist between these three phases: liquid–solid (ls), solid–vapor (sv), and liquid–vapor (lv) interfaces. If we denote the interfacial energies attributed to the three interfaces as σ_{ls}, σ_{sv} and σ_{lv}, respectively, wettability is determined from the interrelation between these three interfacial energies.

In the first place, if the liquid does not wet the surface in the sense demonstrated in Fig. 4, the balance of three interfacial forces (which are identical to the corresponding interfacial energies) leads to the following relation (see Fig. 6):

$$\sigma_{sv} - \sigma_{ls} = \sigma_{lv} \cos\theta \tag{1}$$

where θ is called the contact angle, which is the angle made by the liquid–solid interface and liquid–vapor interface at the point where the three interfaces meet. It is important that the angle should be measured inside (not outside) the liquid phase. Equation (1) is usually called Young's equation. Although Eq. (1) seems quite reasonable, it is not so simple. In the first place, it seems that the contact angle is determined uniquely if three substances (solid, liquid and vapor) and their thermodynamical conditions (temperature, pressure, etc.) are specified. This is not true. The contact angle takes a seemingly arbitrary value between two extremes called the receding contact angle and the advancing contact angle, respectively (Fig. 7). The change of the contact angle between these two values is called hysteresis, the cause of which is not fully understood. Second, from a microscopic point of view, the three phases do not form a point (or line) of contact as shown in Fig. 6. A balance of forces considered within an area a few molecular thicknesses from the geometrical point of

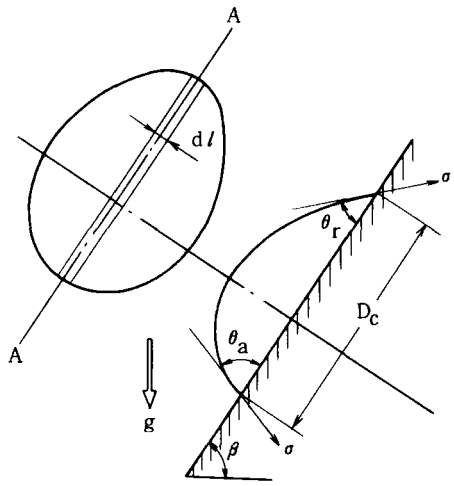

FIG. 7. Hysteresis of contact angle.

contact may be different from that given by Eq. (1). It should be understood that Eq. (1) holds for a finite virtual volume taken around the point of contact. Let us proceed with our discussion, suspending these issues for the present.

When a cap-shaped drop resides on the surface as shown in Fig. 6, the adhesive force F_a between the liquid and solid is derived from a thought experiment as illustrated in Fig. 8:

$$F_a = \sigma_{sv} + \sigma_{lv} - \sigma_{ls} \tag{2}$$

where the first two terms on the right-hand side represent the interfacial energies corresponding to newly formed interfaces and the third term is for the interfacial energy corresponding to the vanished interface. If we substitute Eq. (1) into Eq. (2) we obtain

$$F_a = \sigma_{lv}(1 + \cos\theta) \tag{3}$$

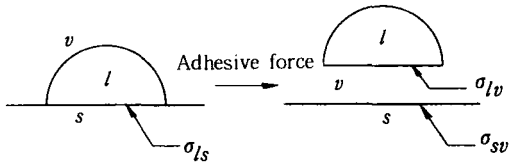

FIG. 8. Adhesive force.

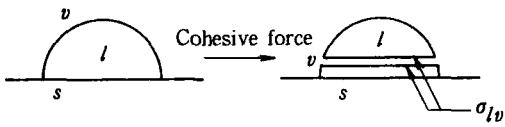

FIG. 9. Cohesive force.

This equation shows that $F_a = 0$ when $\theta = 180°$, which corresponds to the situation that the drop has no affinity at all with the solid surface. A drop of mercury on a glass plate shows a characteristic just like this.

On the other hand, the cohesive force F_c due to the intermolecular attraction is derived by considering a situation as shown in Fig. 9. If the adhesive force holding the liquid against the solid surface is too strong to release the drop from the surface, the drop may be broken inside, as illustrated. If this happens, two liquid–vapor interfaces are formed anew. Thus, the cohesive force is

$$F_c = 2\sigma_{lv} \tag{4}$$

The criterion for the spreading of the liquid drop depends on which one of the two forces, F_a or F_c, is the larger. From Eqs. (2) and (4), the spreading force F_s is defined as follows:

$$F_s = F_a - F_c = \sigma_{sv} - \sigma_{lv} - \sigma_{ls} \tag{5}$$

The spreading force also represents the energy needed to reduce the unit area of the solid–liquid interface. Substitution of Eq. (1) (Young's equation) into Eq. (5) gives

$$F_s = \sigma_{lv}(\cos\theta - 1) \tag{6}$$

When the drop does not spread over the surface, $F_s < 0$, because $|\cos\theta| \leq 1$ and $0 < \theta \leq 180°$. If $\theta = 0$, then $\cos\theta = 1$ and $F_s = 0$, representing the situation that the liquid spreads over the surface without having a finite contact angle. Although any contact angle θ fails to yield $F_s > 0$, it is possible if the solid–vapor interfacial energy σ_{sv} is sufficiently large in Eq. (5). This situation also permits the liquid to spread over the surface. In the ideal situation, the liquid spreads until it forms a monomolecular layer.

As stated above, whether the liquid wets the surface or not is dependent upon the size of the three interfacial energies. However, there are a couple of issues to be noted. First, two out of the three interfacial energies, σ_{sv} and σ_{ls}, are difficult to measure. Both of these are energies on the solid surface. But the characteristics of the solid surface change often, depending on how the surface

is processed (machined, ground, rolled, heat treated, etc.) and on adsorption of foreign substances. To specify the proper characteristics of the surface is very difficult.

Second, in connection with the above, the characteristics of the interface are determined by the state of the molecules within the thickness of a monolayer or, at the maximum, a few molecular layers. This fact is important with regard to the method of promotion of dropwise condensation, which will be discussed later. To sum up, the interrelation between the interfacial energies, which makes the liquid wet the surface or not, is theoretically clear, but in reality it is not. In many cases, it is difficult to know in advance, when the vapor of a certain substance condenses on the surface of some material, which one of the two types of condensation occurs.

To speak very roughly, vapor of pure water condenses filmwise on clean metal surfaces. To cause dropwise condensation of steam on the metal surface, we have to cover the surface with a thin layer of a foreign substance that has a low interfacial energy. To obtain dropwise condensation of an organic vapor, such as freon, is much more difficult because of the very low surface tension of the liquid phase. A substance that causes dropwise condensation is called a promoter. Substances that are effective as promoters will be mentioned in Section IV.

III. Transport Process at Vapor–Liquid Interfaces

A. INTRODUCTION

When film condensation occurs on a solid surface, the most dominant resistance to heat transfer in most cases is the thermal resistance of the condensate film. The thermal resistance of the condensate film was first analyzed by Nusselt [2] more than 70 years ago, and his work still retains its usefulness. On carrying out the analysis, Nusselt made, both explicitly and implicitly, a lot of assumptions for simplification. His assumptions are that the liquid condensate flows smoothly and steadily due to gravity in laminar flow; there are no noncondensable gases in the vapor phase; no vapor shear force acts on the liquid–vapor interface; momentum terms are negligible; the temperature distribution in the condensate film is linear; transfer of the sensible heat in the liquid film is also negligible, with only the heat transported across the liquid film being the latent heat of condensation released at the liquid–vapor interface; and the temperature of the liquid–vapor interface is equal to the saturation temperature of the vapor. The last assumption is to be discussed later.

Under those assumptions, Nusselt derived formulas for condensation on a vertical flat plate and a horizontal circular tube. The result for the former is

$$h = \frac{\dot{q}}{T_s - T_w} = \sqrt[4]{\frac{g\rho_l^2 k_l^3 h_{fg}}{4\mu_l(T_s - T_w)z}} \tag{7}$$

where h is the local heat transfer coefficient at a distance z from the top of the plate (see nomenclature at the end of this article for the rest of the symbols). Forty years after Nusselt's work, Rohsenow *et al.* [7,8] modified the analysis, including the effect of the buoyancy force acting on the liquid film, transfer of the sensible heat in the condensate flow, and nonlinear distribution of the temperature in the condensate layer, with the following result:

$$h = \sqrt[4]{\frac{g\rho_l(\rho_l - \rho_v)k_l^3 h_{fg}[1 + 0.68(c_l \Delta T/h_{fg})]}{4\mu_l(T_s - T_w)z}} \tag{8}$$

where $\Delta T = T_s - T_w$.

Comparison of Eqs. (7) and (8) indicates that the effect of the buoyancy force is a change from ρ_l to $\rho_l - \rho_v$, which is significant only near the critical pressure. The effects of the transport of sensible heat and the nonlinear temperature distribution cause a change of h_{fg} to $h_{fg}[1 + 0.68(c_l \Delta T/h_{fg})]$. This also is a small effect for most applications, because the additional term in the blanket, $0.68(c_l \Delta T/h_{fg})$, remains small as long as the Prandtl number of the liquid is not too small. For low-Prandtl-number liquids, to which liquid metals correspond, both the effects of the momentum change in the liquid film and the nonlinear temperature distribution become important, and the deviation from the modified Nusselt equation becomes larger, as shown in Fig. 10 [9,10]. However, in most applications the magnitude of $(c_l \Delta T/h_{fg})$ is in the lower range and the simple Nusselt formula is usable.

Other factors that change the heat transfer coefficient are the vapor shear force and the noncondensable gases. The former tends to increase and the latter to decrease the heat transfer coefficient (for discussion, see Section V).

Generally speaking, the simple Nusselt analysis agrees rather well with experimental data obtained for film condensation of nonmetal vapors, if proper account for various effects is taken whenever necessary. However, the situation is quite different insofar as condensation of a metal vapor is concerned. This is related to the assumption in defining the heat transfer coefficient that the temperature at the liquid–vapor interface equals the saturation temperature of the vapor. This assumption, of course, is false, and leads to a big error when condensation of a metal vapor at low pressures is to be dealt with.

The assumption that the temperature at the liquid–vapor interface exactly equals the saturation temperature of the vapor seems doubtful if we imagine a

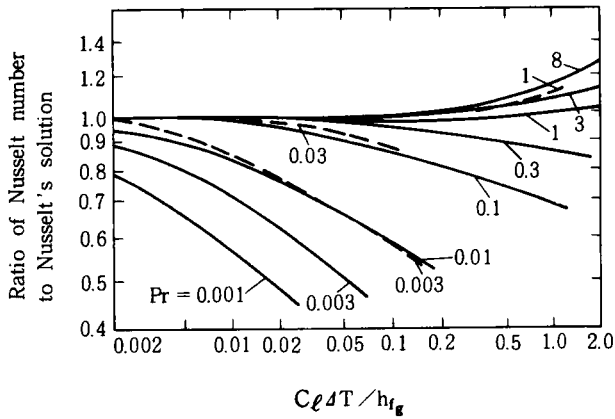

FIG. 10. Effect of the Prandtl number on the heat transfer coefficient of film condensation. (—), Stagnant vapor, vertical plate. From Chen [10]; (--), $\tau = 0$, vertical plate and horizontal tube. From Sparrow and Gregg [9].

situation wherein a vapor and a liquid layer, both of which are at the saturation temperature, coexist. In this case, both of the phases are in thermal equilibrium and no heat should be transferred between the two. If we observe microscopically, there might be transport of molecules crossing the liquid–vapor interface in both directions, as discussed in Section II. However, this does not cause any net condensation or evaporation, and the state of thermal equilibrium continues. The situation is similar when the condensate surface with the saturation temperature faces the saturated vapor. No net condensation must take place under such a condition. For net condensation to occur there should be a finite amount of difference between the saturation temperature of the vapor, T_s, and the temperature of the liquid–vapor interface, T_i. As will be made clear, the difference between T_s and T_i is not so large for nonmetal vapors except at very low pressures, but for metal vapors the difference can be large. This is schematically depicted as in Fig. 11. If T_s differs from T_i appreciably, the condensation heat transfer coefficient based on $(T_s - T_w)$, as in Eq. (7) or (8), will not predict a true value.

B. THEORY OF INTERPHASE MASS TRANSFER

According to the kinetic theory of gases, the statistical behavior of a gas at a certain temperature is described by an appropriate velocity distribution function. If the gas is in a uniform steady state, so that its macroscopic properties do not vary with time or position, then the function known as

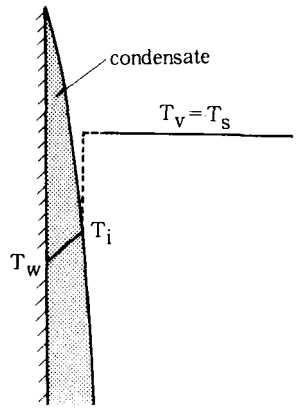

FIG. 11. Temperature distribution in vapor and liquid film in condensation of metal vapor.

the Maxwell velocity distribution is derived. If we denote the three velocity components of the gas molecule in Cartesian space by U, V, and W, the Maxwell velocity distribution function is expressed as

$$f = n\left(\frac{1}{2\pi RT}\right)^{3/2} \exp\left\{-\frac{1}{2RT}(U-\bar{U})^2 + (V-\bar{V})^2 + (W-\bar{W})^2\right\} \quad (9)$$

where R is the gas constant, and $\bar{U}$, $\bar{V}$, and $\bar{W}$ are the components of the mean linear velocity due to global mass motion of the total system.

Schrage [11] used this Maxwellian distribution kinetic theory to analyze the mass transfer process at the liquid–vapor interface. As will be mentioned later, Schrage's analysis is rather easy to understand, but is based on a few assumptions for simplification. Some modifications have been made by other researchers. An article by Rohsenow [12] gives a compact summary of those works.

If the velocity of vapor molecules obeys the Maxwell distribution, the rate of net condensation $\dot{m}$ per unit area is expressed by the following relation:

$$\dot{m} = \sigma_c \Gamma \frac{P_v}{\sqrt{2\pi RT_v}} - \sigma_e \frac{P_i}{\sqrt{2\pi RT_i}} \quad (10)$$

where

$$\Gamma \simeq 1 + \frac{\dot{m}}{P_v\sqrt{2/(\pi RT_v)}} \quad (11)$$

Here, the first term on the right-hand side of Eq. (10) (without $\sigma_c\Gamma$) represents the mass flux of molecules from the vapor phase that impinge on the surface.

The coefficient σ_c, the condensation coefficient, represents the fraction of molecules captured by the liquid. The term Γ corresponds to the fact that the vapor as a whole progresses toward the surface as long as net condensation takes place. This "progress" velocity should be superimposed on the Maxwell velocity distribution. In Eqs. (10) and (11), P_v is the vapor pressure at the liquid surface and is assumed to be the saturation pressure corresponding to T_v and to be identical with the pressure of the system. The second term of Eq. (10) (without σ_e) represents the emission from the liquid surface at a uniform temperature T_i. P_i here is the saturation pressure corresponding to T_i. The coefficient σ_e, the evaporation coefficient, represents the fraction of molecules that actually leave the surface. It is assumed that the emission of molecules from the liquid surface is not affected by the higher pressure in the vapor when net condensation is occurring.

Substitution of Eq. (11) into Eq. (10) gives

$$\dot{m} = \frac{2}{2 - \sigma_c}\left(\sigma_c \frac{P_v}{\sqrt{2\pi R T_v}} - \sigma_e \frac{P_i}{\sqrt{2\pi R T_1}}\right) \tag{12}$$

If we assume that the condensation coefficient is equal to the evaporation coefficient and is simply denoted σ, Eq. (12) becomes

$$\dot{m} = \frac{2\sigma}{2 - \sigma} \frac{1}{\sqrt{2\pi R}}\left(\frac{P_v}{\sqrt{T_v}} - \frac{P_i}{\sqrt{T_i}}\right) \tag{13}$$

It should be noted here that there is no theory that has proved or disproved that the assumption that $\sigma_c = \sigma_e$ is correct whenever net condensation or evaporation takes place. Of course, the assumption must be valid at an equilibrium state when $T_v = T_i$, because no mass transport should occur. However, let us suspend our doubt for the present.

Equation (13) can be put into the following form if we assume $(T_v - T_i)/T_v \ll 1$, which is valid except when the vapor temperature is very low:

$$\dot{m} = \frac{2\sigma}{2 - \sigma} \frac{P_v}{\sqrt{2\pi R T_v}}\left(\frac{P_v - P_i}{P_v} - \frac{T_v - T_i}{2T_v}\right) \tag{14}$$

When the two terms in the parentheses on the right-hand side of Eq. (14) are compared, the first term, $(P_v - P_i)/P_v$, is usually much larger than the second term, $(T_v - T_i)/(2T_v)$. Even for pressure as low as 0.1 kPa for both metal vapors and for water vapor, the second term is around 3–4% of the second. At higher pressures this relative magnitude is much smaller. Thus, if we neglect the second term, Eq. (14) is written as

$$\dot{m} = \frac{2\sigma}{2 - \sigma} \frac{P_v - P_i}{\sqrt{2\pi R T_v}} \tag{15}$$

Further, from the Clausius–Clapeyron relation

$$\frac{P_v - P_i}{T_v - T_i} \approx \frac{\rho_v h_{fg}}{T_v} \tag{16}$$

If this approximation is employed, Eq. (15) becomes

$$\dot{m} = \frac{2\sigma}{2 - \sigma} \frac{h_{fg}}{\sqrt{2\pi R}} \frac{\rho_v (T_v - T_i)}{T_v^{3/2}} \tag{17}$$

Here, let us convert the rate of condensation $\dot{m}$ into the heat flux using the relation

$$\dot{q} = h_{fg} \dot{m} \tag{18}$$

Then Eq. (17) becomes

$$\dot{q} = \frac{2\sigma}{2 - \sigma} \frac{h_{fg}^2}{\sqrt{2\pi R}} \frac{\rho_v (T_v - T_i)}{T_v^{3/2}} \tag{19}$$

Or we can derive from Eq. (19) an apparent heat transfer coefficient at the liquid–vapor interface, h_i:

$$h_i = \frac{\dot{q}}{T_v - T_i} = \frac{2\sigma}{2 - \sigma} \frac{h_{fg}^2 \rho_v}{\sqrt{2\pi R T_v^3}} \tag{20}$$

We should note that this interfacial heat transfer coefficient is defined for the temperature difference $(T_v - T_i)$. It means that the total resistance to condensation heat transfer can be written as

$$\frac{1}{h} = \frac{1}{h_f} + \frac{1}{h_i} \tag{21}$$

where $(1/h_f)$ is the thermal resistance due to the liquid film and h_f is expressed by Eq. (7) or (8).

The interfacial heat transfer coefficient, or the temperature "jump" at the liquid–vapor interface $(T_v - T_i)$ can be obtained from Eq. (20), if we assume the value of σ.

Shown in Table I are the interfacial heat transfer coefficients h_i and the vapor-to-interface temperature differences, calculated for three vapors at different pressures under the condition of a constant vapor-to-wall temperature difference, i.e., $T_v - T_w = 10$ K. The condensation coefficient is assumed to be unity. It is known that the interfacial heat transfer coefficient of water vapor at atmospheric pressure is extremely high, being almost three orders of magnitude higher than the heat transfer coefficient of film condensation. This is the cause of the high heat transfer rate of dropwise condensation. The

TABLE I

INTERFACIAL HEAT TRANSFER COEFFICIENTS AND TEMPERATURE DROPS FOR VARIOUS VAPORS[a]

Property	Substance							
	Water			Sodium			Potassium	
Molecular mass M (kg/kmol)	18.052			22.99			39.098	
Gas constant R (J/kg K)	461.5			361.7			212.65	
Vapor pressure P_v (atm)	1.0	0.1	0.01	1.0	0.1	0.01	1.0	0.01
Vapor temperature T_v (K)	373.15	319.24	280.32	1154.6	949.1	806.7	1029.7	697.4
Vapor density ρ_v (kg/m^3)	0.598	0.0690	0.00783	0.270	0.0315	0.00361	0.504	0.00699
Interfacial heat transfer coefficient h_i (MW/m^{2}K)	15.7	2.57	0.383	5.74	0.771	0.117	3.71	0.100
Interfacial temperature drop $T_v - T_i$(K)	0.007	0.037	0.18	0.33	2.3	7.3	0.30	6.3
Temperature drop in condensate $T_i - T_w$(K)	9.99	9.96	9.82	9.67	7.7	2.7	9.70	3.7

[a] Calculations are carried out under a vapor-to-surface temperature difference $T_v - T_w = 10$ K. Thermal properties are from Refs. [128–132].

interfacial temperature drops for water vapor are relatively small, whereas those for metal vapors are much larger, especially when the pressure is low.

C. MODIFICATION OF SCHRAGE'S THEORY

There have been a number of attempts to improve Schrage's result. Some of these are referred to in the following discussion.

Huang [13] has considered that molecules impinging on the surface at low grazing angles are not captured. His analysis has led to the following result:

$$\dot{m} = \frac{\pi}{2} \frac{P_v}{\sqrt{2\pi R T_v}} \left(\frac{P_v - P_i}{P_v} - \frac{T_v - T_i}{2T_v} \right) \tag{22}$$

If Eq. (22) is compared with Eq. (14), the only difference is that $2\sigma/(2 - \sigma)$ in Eq. (14) is replaced by $\pi/2$ in Eq. (22). This means that Eq. (22) is identical with Eq. (14) only if $\sigma = 2\pi/(4 + \pi) = 0.880$, which is equivalent to say that the upper limit of σ in Schrage's equation should be 0.88. However, Huang's assumption that molecules at a small grazing angle are not captured has not been verified either theoretically or experimentally.

Springer and Patton [14] presented an analysis using the double-flow distribution function and the moment method and obtained the following result:

$$\dot{m} = \frac{P_v}{\sqrt{2\pi R T_v}} \left[\frac{\dfrac{\sigma_e}{\sigma_c} \dfrac{\Delta P}{P_v} - \dfrac{1}{2} \dfrac{\Delta T}{T} \left(\dfrac{1}{1 + 4/15\mathrm{Kn}} + \dfrac{\sigma_e}{\sigma_c} - 1 \right) - \dfrac{\sigma_e}{\sigma_c} + 1}{\dfrac{2 - \sigma_c}{2\sigma_c} + \dfrac{1}{2 + 8/15\mathrm{Kn}}} \right] \tag{23}$$

where Kn is the Knudsen number, which is the ratio of the mean free path of the molecules to some characteristic length. Because all available data for the condensation coefficient have been taken at pressures where the Knudsen number is almost zero, Eq. (23) is identical with Schrage's equation in most of the cases.

Labuntzov [15] reported an analysis also using the double-flow distribution function. His result, which is valid for near-equilibrium condensation, can be written as

$$\dot{m} = \frac{2\sigma}{2 - 0.798\sigma} \frac{P_v - P_i}{\sqrt{2\pi R T_v}} \tag{24}$$

The term involving the coefficient σ is a little different from that in Eq. (15). If the σ coefficients in Eqs. (14) and (23) are distinguished by subscripts S and L,

respectively, and equating the both terms, we get

$$\sigma_S = 0.798\sigma_L \tag{25}$$

This means that Schrage's coefficient σ_S is about 80% of Labuntzov's σ_L.

Labuntzov and Kryukov [16] have revised the analysis, taking into consideration a unique character of the nonequilibrium state of vapor near the liquid–vapor interface, where the Knudsen number is finite. They used a model of the interface region in which the liquid surface and the uniform gas are separated by a "Knudsen layer" and a "gas-dynamic flow region." They treated the former region by solving approximately the Boltzmann equation and the latter region on the basis of the continuum mechanics, and derived a formula that described the process of intensive condensation as follows:

$$\dot{m} = 1.67\frac{P_v - P_i}{\sqrt{2\pi RT_v}}\left\{1 + 0.515\ln\left[\frac{P_v}{P_i}\left(\frac{T_i}{T_v}\right)^{\frac{1}{2}}\right]\right\} \tag{26}$$

In deriving this formula, the condensation coefficient is taken as unity. A big difference between this equation and the equations mentioned before is that the term multiplied by $(P_v - P_i)/\sqrt{2\pi RT}$ is not constant in Eq. (26) whereas it is constant in the other equations, such as Eqs. (15) and (24). It seems that, at present, Eq. (26) is the most reliable equation for describing mass transfer at the liquid–vapor interface, but only if the condensation coefficient is actually very close to unity.*

D. EXPERIMENTAL DETERMINATION OF CONDENSATION COEFFICIENT

Both the condensation and the evaporation coefficients have been measured in a variety of experiments. Table II summarizes the previous experimental values for the condensation coefficient of water vapor. Very low (0.006) to very high (1.0) values have been reported.[1]

Shown in Fig. 12 [20] is the dependence of the condensation coefficient of metal vapors on the system pressure. Although the degree of scatter of the data is considerable, it looks as though there is a tendency for the condensation coefficients to be close to unity when the pressure is low, and to decrease as the pressure increases. Wilcox and Rohsenow [20] considered that

* The condensation mass flux for the arbitrary value of the condensation coefficient is given in Labuntzov [15], but is not shown here.

[1] Most of Table II is from Mills and Seban [17]. The only exceptions are the results by Narusawa and Springer [18] and Hatamiya and Tanaka [19].

TABLE II

EXPERIMENTAL VALUES FOR CONDENSATION/EVAPORATION COEFFICIENT OF WATER

Investigators[a]	Temperature (°C)	σ	Nature of the experiment
Alty (*1*)	18 ~ 60	0.006 ~ 0.016	evaporation from a suspended drop
Alty and Nicoll (*2*)	18 ~ 60	0.01 ~ 0.02	Evaporation from a suspended drop
Alty (*3*)	−8 ~ +4	0.04	Evaporation from a suspended drop
Alty and Mackay (*4*)	15	0.036	Evaporation from a suspended drop
Pruger (*5*)	100	0.02	Evaporation from a horizontal surface
Hammecke and Kappler (*6*)	20	0.045	Evaporation from a horizontal surface
Hammecke and Kappler (*7*)	?	0.100	Evaporation from a horizontal surface
Delany *et al.* (*8*)	0 ~ 43	0.0415 ~ 0.0265	Evaporation from a horizontal surface
Narusawa and Springer [18]	19 ~ 27	0.038 ~ 0.2	Evaporation from a horizontal surface
Hickman (*9*)	0	0.42	Evaporation from a tensimeter jet
Navabian and Bromley (*10*)	10 ~ 50	$0.35 \leq \sigma \leq 1.0$	Film condensation on a fluted tube
Jamieson (*11*)	0 ~ 70	0.35	Condensation on a tensimeter jet
Berman (*12*)	?	Near 1.0	Film condensation on a horizontal cylinder
Hatamiya and Tanaka [19]	7 ~ 27	$0.2 \leq \sigma \leq 0.6$	Dropwise condensation on a flat plate

[a] *References* provided here are not given in the general reference list: (*1*) *Proc. R. Soc. London, Ser. A* **131,** 554 (1931); (*2*) *Can. J. Res.* **4,** 547 (1931); (*3*) *Philos. Mag.* **15,** 82 (1933); (*4*) *Proc. R. Soc. London, Ser. A* **149,** 104 (1935); (*5*) *Z. Phys.* **115,** 202 (1940); (*6*) *Z. Geophys.* **19,** 181 (1953); (*7*) *Verk. Minist. N. Rhein-Westf.* **3,** 125 (1955); (*8*) *Chem. Eng. Sci.* **19,** 105 (1964); (*9*) *Ind. Eng. Chem.* **46,** 1442 (1954); (*10*) *Chem. Eng. Sci.* **18,** 651 (1963); (*11*) *Symp. Thermophys. Prop., 3rd, Purdue Univ., Lafayette, Indiana* p. 230 (1965); (*12*) *Khim. Mashinostr.* No. **36,** 66 (1961).

the apparent decrease of the condensation coefficient with the increase of pressure was due to a lack of precision of measurement.

In determining the condensation coefficient σ, the method most commonly employed is to measure the heat flux and the surface temperature at the condensing surface, then to derive the temperature of the liquid–vapor interface from Eq. (8) (by replacing T_s by T_i), and finally, using Eq. (19) or another

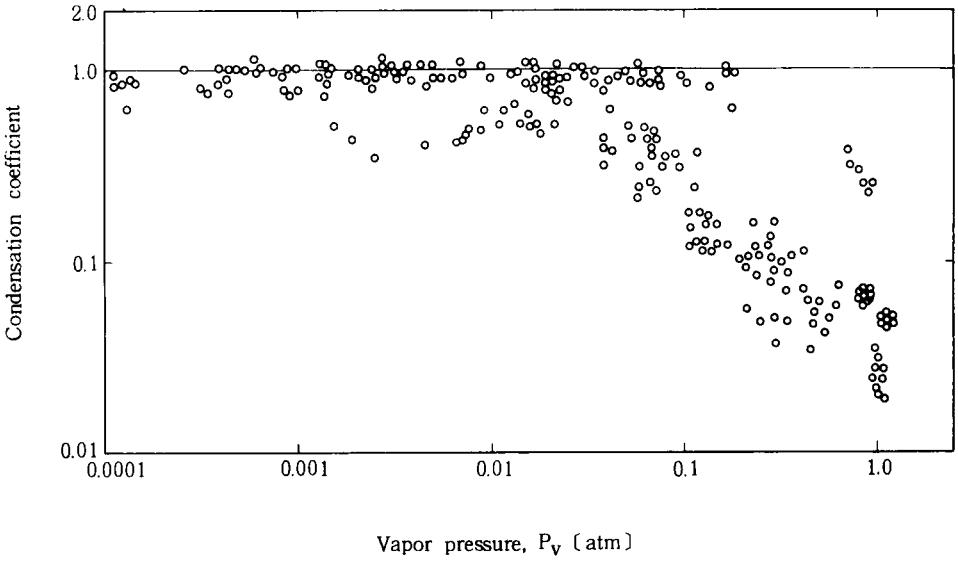

FIG. 12. Condensation coefficient data.

appropriate equation, to calculate σ. The major cause of error is in the determination of $T_v - T_i$. At a given heat flux $\dot{q}$, the temperature difference $T_v - T_i$ decreases rapidly to a very small value as pressure increases. As illustrated in Table I, the vapor-to-interface difference $T_v - T_i$ is of the order of, or less than, 1 K when the pressure exceeds 0.1 atm. Because some inaccuracies in the determination of heat flux and temperatures T_v and T_i are inevitable, it may be very difficult to obtain $T_v - T_i$ with high precision at higher pressures.

Wilcox and Rohsenow [20] discussed the accuracy of measurement in determining the condensation coefficient of metal vapor. In most experiments the heat fluxes and the surface temperatures are obtained by measuring the temperature distribution in the heat transfer block and extrapolating the readings of several positions to the surface. They have postulated a Gaussian distribution in error that is related to the thermocouple hole size at each location. They have presented a relation for the standard deviation in the determination of the value of the surface temperature T_w. This standard deviation is dependent on the hole size, the number and spacing of the holes, and the thermal conductivity of the block. The standard deviation is reduced by using a highly conductive solid as the block material, a smaller diameter, and a greater number of thermocouple holes.

Shown in Table III is an example of the standard deviation in the determination of T_w for three different block materials [12]. The standard

TABLE III

STANDARD DEVIATIONS IN THE DETERMINATION OF WALL TEMPERATURE[a]

Material of the condensing block	Number of holes	Diameter of holes (mm)	Standard deviation (°C)
Copper	6	1.2	0.13
Nickel	3	1.6	1.6
Stainless steel	3	1.6	14.4

[a] $\dot{q} = 150\,\mathrm{kW/m^2}$.

deviation $(T_w - \bar{T}_w)$ is larger, if the number of thermocouple holes is reduced and the block material has poorer thermal conductivity. Comparison of Tables I and III suggests that we could hardly trust the values of condensation coefficients obtained at pressures higher than, say, 0.3 atm. Wilcox and Rohsenow have concluded that, taking into account the limitation of precision of measurement, the magnitude of the condensation coefficient is quite high—very close to unity.

The present author considers that the manner in which Wilcox and Rohsenow reached their conclusion was intuitive rather than logical, though the conclusion might still be somewhat valid. However, very recently stronger experimental evidence has been presented by Ishiguro and Sugiyama [21], who, as a result of a very elaborate experimental study, have determined that the value of the condensation coefficient of potassium vapor is substantially unity, in the sense that Labuntzov and Kryukov [16] have defined it. Figure 13 shows their experimental apparatus. They took great care to avoid inaccuracies due to (1) errors caused by measurement of the heat flux and the surface temperature of the condensing surface, (2) errors in measuring the vapor pressure, (3) the effect of noncondensable gases, and (4) inconsistencies between the analytical model and the actual process.

Shown in Fig. 14 is the result of the measurement. The variable ξ on the ordinate is defined as follows:

$$\dot{m} = \xi \frac{P_v - P_i}{\sqrt{RT_v}} \tag{27}$$

Comparison of Eq. (27) with Eq. (15) gives

$$\xi = \frac{1}{\sqrt{2\pi}} \frac{2\sigma_s}{2 - \sigma_s} \tag{28}$$

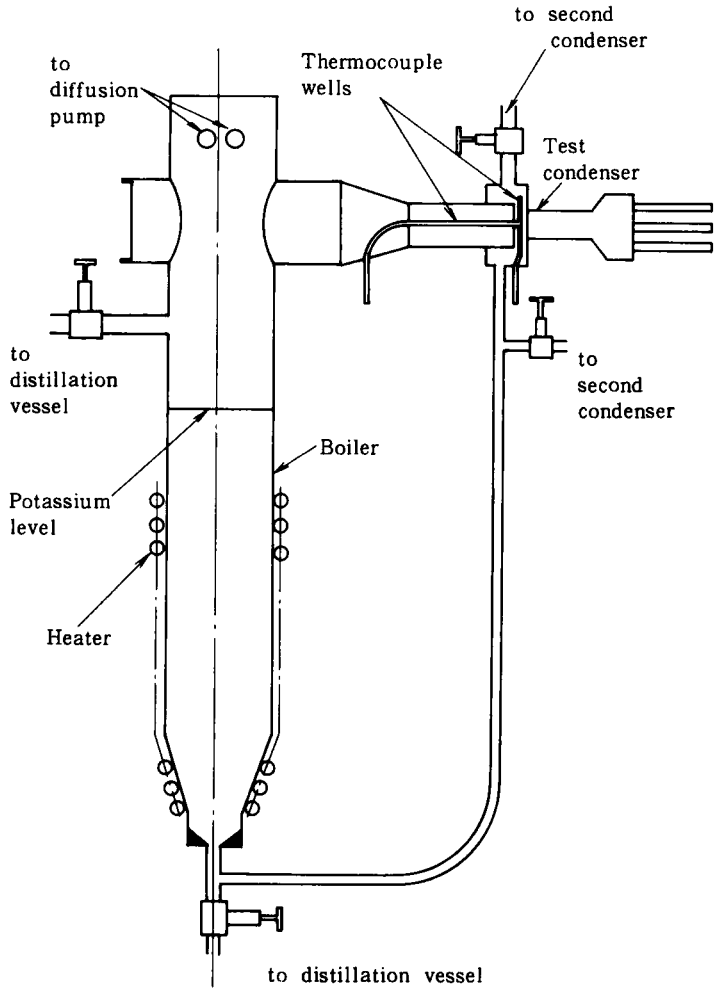

FIG. 13. Experimental apparatus by Ishiguro and Sugiyama [21].

In this case ξ takes a constant value. On the other hand, if comparing with Eq. (26), it follows that

$$\xi = \frac{1.67}{\sqrt{2\pi}}\left\{1 + 0.515 \ln\left[\frac{P_v}{P_i}\left(\frac{T_i}{T_v}\right)^{1/2}\right]\right\} \tag{29}$$

where the condensation coefficient is assumed to be unity.

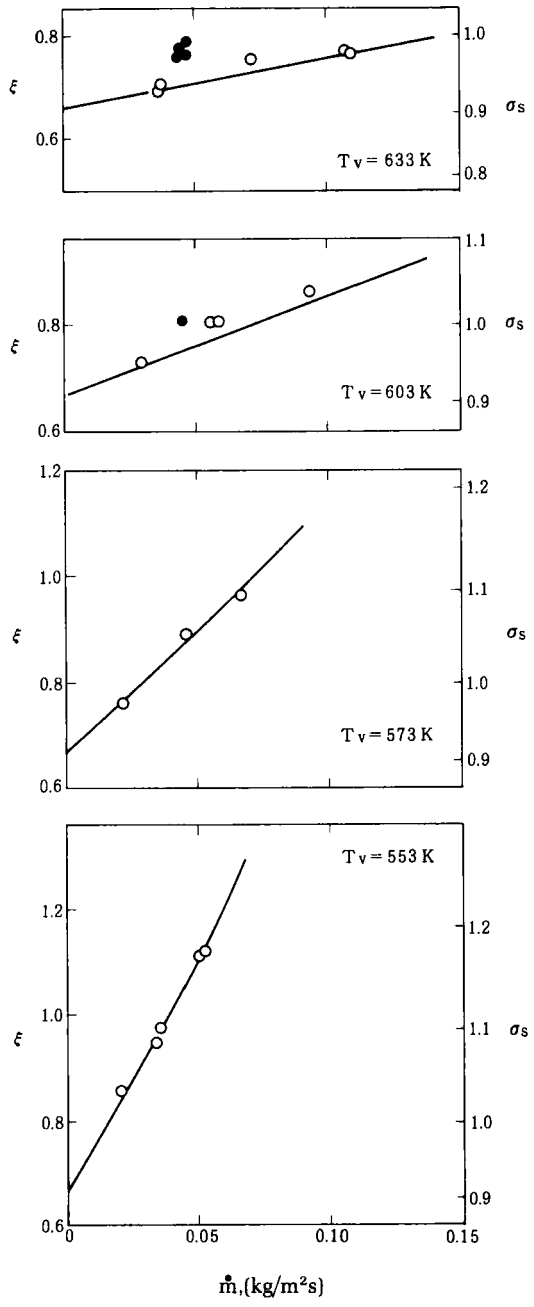

FIG. 14. Dependence of ξ [defined by Eq. (27)] on condensation mass flux. (○), Present result; (—), Labontsov and Kryukov ($\sigma = 1$); (●), Subbotin *et al.*

The experimental results shown in Fig. 14 indicate that they all agree fairly well with the theory by Labuntzov and Kryukov. It means that the variable ξ is dependent on the condensation mass flux $\dot{m}$, while Schrage's theory yields a constant ξ as expressed by Eq. (28). If a state very near to equilibrium, that is to say, $\dot{m} \cong 0$, is considered, the Labuntzov–Kryukov theory gives a value $\xi = 0.67$, whereas $\xi = 0.8$ by Schrage's theory, assuming $\sigma_s = 1$. This means that the rate of condensation derived by Schrage's equation is 1.19 times larger than that by the Labuntzov–Kryukov equation. The cause of this difference lies in the fact that the collision between the vapor molecules and the molecules emitted from the liquid phase is taken into consideration in the Labuntzov–Kryukov analysis, whereas such an interference is not considered by Schrage.

Note in Fig. 14 that the variable ξ increases with $\dot{m}$. This can be explained by considering the interference between the oncoming molecules and the departing molecules as described above. As the temperature of the vapor phase increases, the average momentum possessed by the emitted molecules becomes relatively smaller than the average momentum of the condensing vapor molecules, which prevent the molecules in the liquid layer from leaving. On the other hand, the effect of such an interaction becomes smaller as the temperatures of the phases converge. Similar conclusions were also reported by Necmi and Rose [22] and Niknejad and Rose [23] as the result of experiments on the condensation of mercury vapor. However, their results differed a little from the analysis by Labuntzov and Kryukov.

It seems that most of the experimental results published recently indicate that the condensation coefficient is close to unity in the case of condensation of a metal vapor, though there is a little difference among the formulas describing the process of interfacial mass transfer. No studies have reported that the condensation or evaporation coefficient of water vapor is unity. Even very recent experiments have reported the value to be significantly smaller than 1.0. As shown in Table II, Narusawa and Springer [18] reported a value of 0.2 as the evaporation coefficient. Hatamiya and Tanaka [19] have estimated that the value of the condensation coefficient is in the range between 0.2 and 0.6, the most probable value being 0.4, from the result of an experiment on the dropwise condensation of low-pressure steam. That the condensation coefficient of water vapor is significantly smaller than unity is supported by some and doubted by others.

Fujikawa and Maerefat [24] have discussed this problem on the basis of the transition-state theory of statistical mechanics. They insist that the condensation coefficient of a polyatomic fluid should be significantly smaller than 1.0 because the rotational motion of molecules in the liquid state is constrained. On the other hand, Stylianou and Rose [25] and Rose [26] suggest, on the basis of work done by Le Fevre [27], that, if polyatomicity of

the water molecule is taken into account, the data on the condensation coefficient should be amended to be closer to unity. For example, the values estimated by Hatamiya and Tanaka, 0.2–0.6, should be shifted to 0.38–0.93.

The present author is not capable of judging which one of these theories is most reasonable. It seems that a much deeper understanding about molecular kinetic processes at the liquid–vapor interface is needed to reach a conclusion.

IV. Dropwise Condensation

A. Microscopic Mechanisms

As described in Section II, dropwise condensation is composed of several processes that are combined randomly both in space and in time. Figure 3, which shows what the author calls the "life cycle" of dropwise condensation, helps to understand the basic nature of the process.

To understand each individual process of the life cycle of dropwise condensation and to know about the interrelationship between them are the most essential aspects of the study of the mechanism of dropwise condensation. It is likely that elaborate work done within the past 25 years has thrown sufficient light on those processes. But on closer examination of each of those studies, it can be concluded that there still remain surprisingly many unanswered questions. Table IV provides a summary of the nature of the problems that remain unresolved. Detailed descriptions of each of the problems will not be given here because of the space limitation. Only a few brief comments will be made below. Interested readers are invited to refer to the author's monographs published elsewhere [28].

1. *Initial Droplet Formation*

Two opposite hypotheses have been proposed as to the mechanism of initial droplet formation: one is the film fracture hypothesis, which was first proposed by Jakob [29] and later supported by Welch and Westwater [30], and the other is the nucleation theory. But since Umur and Griffith [31] have insisted that the continuous growth of film is impossible on a nonwetting surface, and McCormick and Westwater [32] have made supporting microscopic observations, the nucleation hypothesis has been supported by most people. The present author makes no objection to it so long as the nucleation occurs on a completely dried surface. However, in the actual process of dropwise condensation, it might be possible that a very thin film of condensate is left behind in the wake of a departing drop, and from there the initial drops are generated in a somewhat different way. But it does not matter to the macroscopic process of heat transfer whether or not the drops originate by nucleation.

TABLE IV

THINGS NOT KNOWN ABOUT THE MECHANISM OF DROPWISE CONDENSATION

Classification of problems		
Item	Subitem	Supplementary explanation
Initial droplet formation	Mode of formation	Film fracture or nucleation? (Nucleation hypothesis is supported by the most of the researchers, but decisive proof has not yet been given)
	Nucleation site	What parts of the surface can be the nucleation sites? Pits, grooves, extrudes, or defects of promoter layer? (Proof by observation is yet lacking)
	Population density of nucleation site	What is the magnitude? What is the relationship with the surface condition? What is the relationship with the surface subcooling? (Possible relationship with the heat transfer coefficient)
	Critical size for drop growth	Is the critical radius given by the Kelvin–Helmholtz equation correct? (This equation holds only for the thermodymic equilibrium process, whereas the drop growth process is nonequilibrium. Actual observation is necessary)
	Rate of drop formation	How many drops are formed per unit area and per unit time? (Relationship with the nucleation site density and the surface subcooling)
Growth of drop	Growth by condensation	Theoretical analysis of the drop growth process due to condensation is necessary. (Heterogeneity of the surface temperature and its fluctuation should be taken into consideration) Can it be confirmed by the actual observation?
	Growth by coalescence	How much is the drop growth augmented by coalescence? Dynamics of coalescence should be made clear (rate of coalescence, behavior of drop at coalescence) Surface temperature fluctuation due to coalescence should be measured.
Departure of drop	Mechanism of drop departure	What is the cause of the hysteresis of contact angle? Can it be estimated theoretically? Can the departure size be decided theoretically? Departure size should be measured under various conditions What is the relationship between the static and the dynamic departure size?
	Dynamics of drop departure	Behavior of the departing drop, i.e., deformation, sliding velocity, and sweeping process, should be measured and analyzed

2. *Drop Growth*

As already mentioned, it is fruitless to make an attempt to analyze the drop growth process due to condensation exclusive of coalescence. What remains for the future is to measure the rate of drop growth, simultaneously with the local surface temperature fluctuation.

3. *Drop Departure*

To derive theoretically the departure size seems difficult for the time being, because of the yet unsolved phenomenon of "contact angle hysteresis," as shown in Fig. 7. At present, we have no definite theory that can give an explanation for this. More extensive measurement is necessary, and the effects of external forces, surface conditions, and heat flux should be made clear. Once the relationship between the departure size and the external conditions is established, the heat transfer coefficient becomes predictable, as will be discussed later.

B. MEASUREMENT OF HEAT TRANSFER COEFFICIENTS

Experimental studies on the heat transfer by dropwise condensation have been carried out mostly under very limited conditions. It is only recently that the data on the heat transfer coefficient of dropwise condensation of steam at atmospheric pressure have been put in order. Those data for other vapors and measurements under different thermal conditions are still scarce. Therefore, the description that follows is mostly concentrated on dropwise condensation of steam at near-atmospheric pressure.

1. *Results of Measurements on Steam at Near-Atmospheric Pressure*

Since the first observation was made by Schmidt *et al.* [3], the heat transfer coefficient of dropwise condensation of steam near 1 atm has been measured by many other researchers. The results have been summarized by Tanner *et al.* [33], Graham [34], and Tanasawa [28], and show a considerably wide scatter. However, because the experimental techniques have shown great progress, the reproducibility and reliability of the experimental data have been established to some extent. We owe much to the work by Le Fevre and Rose [35,36] and Citakoglu and Rose [37]. At present, we can say that the heat transfer coefficient of dropwise condensation of steam at 1 atm, under normal gravitational acceleration and on a vertical copper surface, is about 250 ± 50 kW/m^2 K, provided that there is no effect of noncondensable gases, the height of the condensing surface is less than about 50 cm, the heat flux is of the order of 0.1–1 MW/m^2, and the steam velocity is less than 10 m/sec.

The variation of the magnitude of the heat transfer coefficient mentioned above is mostly due to the effects of steam velocity and surface characteristics. As several authors have pointed out, the reasons that most of the past measurements reported much lower heat transfer coefficients may be (1) inaccuracy in the measurement of surface temperature and heat flux and (2) carelessness regarding the buildup of noncondensable gases on the condensing surface.

2. *Measurements on Low-Pressure Steam*

Fewer results are available on the heat transfer coefficient of dropwise condensation of steam under pressures lower than 1 atm. Figure 15 shows the data reported by five different groups of researchers [34,38–41]. There is a little difference among groups, but every result shows a tendency of decreasing heat transfer coefficients with decreasing pressures.

3. *Effect of Drop Size*

The heat transfer coefficient of dropwise condensation is dependent upon the distribution of drop sizes on the condensing surface. And what largely

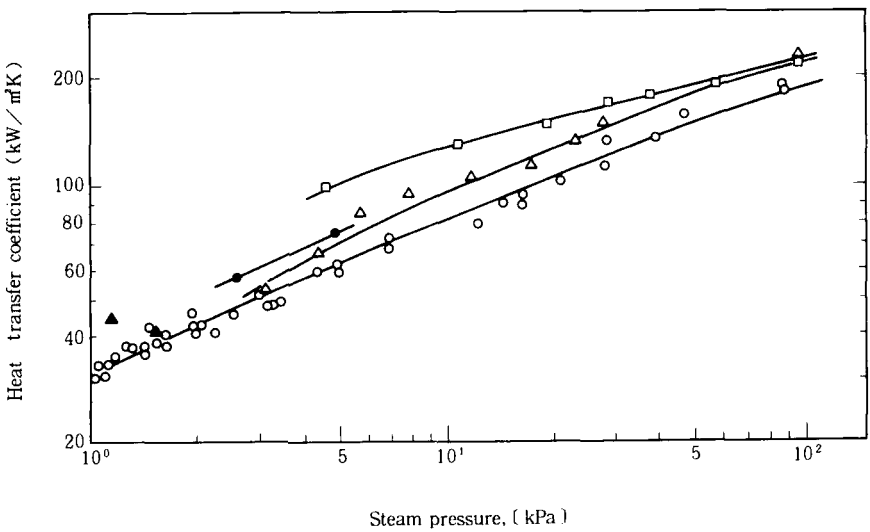

FIG. 15. Dropwise condensation of low-pressure steam. (●), Tanner *et al.* [38]; (△), Graham [34]; (□), Wilmshurst and Rose, [39]; (▲), Tsurta and Tanaka [40]; (○), Hatamiya and Tanaka [41].

determines the drop size distribution is the maximum drop diameter or the departing drop diameter, together with the fraction of the area covered by sliding drops. Thus, the author would like to emphasize that the relationship between the drop size and the heat transfer rate should be studied more intensively. Some of the factors that have an influence upon the heat transfer coefficient of dropwise condensation are closely related to the maximum drop diameter. They are, for example, the vapor velocity, the physical and chemical characteristics of the surface (such as roughness and wettability), and the inclination and the height of the surface.

A number of reports have been published in which the effects of vapor velocity or the height or the inclination of the condensing surface are measured. Drop size measurements were not carried out for the most part, however.

Tanasawa *et al.* [42] measured the dependence of the heat transfer coefficient on the departing drop diameter, using the gravitational, centrifugal, and steam shear forces to change the departing drop diameter. The result is shown in Fig. 16. It has been found that, no matter what kind of force may be used to prompt drop departure, the heat transfer coefficient is proportional to the departing drop diameter to the power of about -0.3. It is very interesting to note that Tanaka [43,44] and Rose [45] have theoretically derived quite similar conclusions.

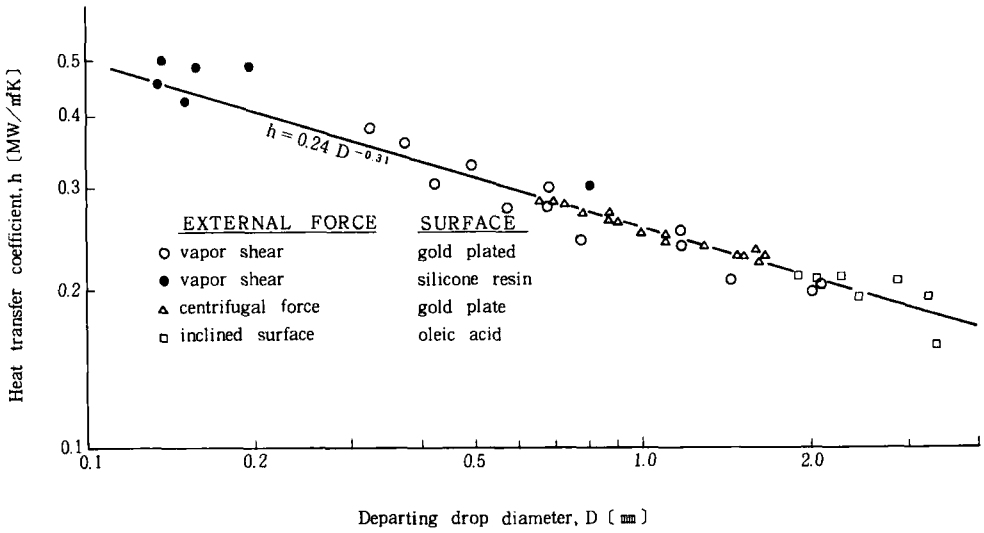

FIG. 16. Dependence of heat transfer coefficient of dropwise condensation on departing drop diameter.

4. *Condensation Curves*

In pool boiling, it is well known that the mode of heat transfer shifts from convection to nucleate boiling, then to transition boiling, and finally to film boiling, with the increase in the degree of surface superheat. The heat flux also varies with the superheat. The curve that represents the change of heat flux with the superheat is called the boiling curve and was first obtained by Nukiyama [46]. In dropwise condensation, a similar curve, which may be called a "condensation curve," must be obtained. In the case of the condensation curve, however, it was very difficult to realize a large surface subcooling.

The first measurement of condensation curves on steam at atmospheric pressure was carried out by Takeyama and Shimizu [47]. However, there was some doubt about the accuracy of their measurement. Tanasawa and Utaka [48] made measurements with much greater accuracy using a condensing surface with a special configuration of a concave sphere (Fig. 17). The results are shown in Fig. 18, with the result obtained by Takeyama and Shimizu included as a thin, solid line. It is seen that the shapes of the condensation curves are similar to those of the boiling curves, whereas the maximum heat fluxes are higher, exceeding 10 MW/m^2. Dropwise condensation is maintained from a lower degree of surface subcooling up to the maximum heat flux. At a much larger surface subcooling, the condensate begins to accumulate on part of the condensing surface and a state of pseudofilm condensation is observed. When the surface temperature is lowered below 0°C, a layer of ice is formed on the surface and film condensation occurs on the layer (on-ice condensation).

One of the important conclusions derived from this experiment is that dropwise condensation continues up to a considerably larger heat flux. This

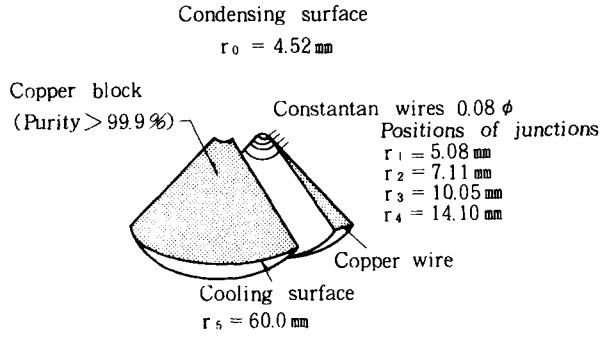

FIG. 17. Heat transfer block with a concave condensing surface.

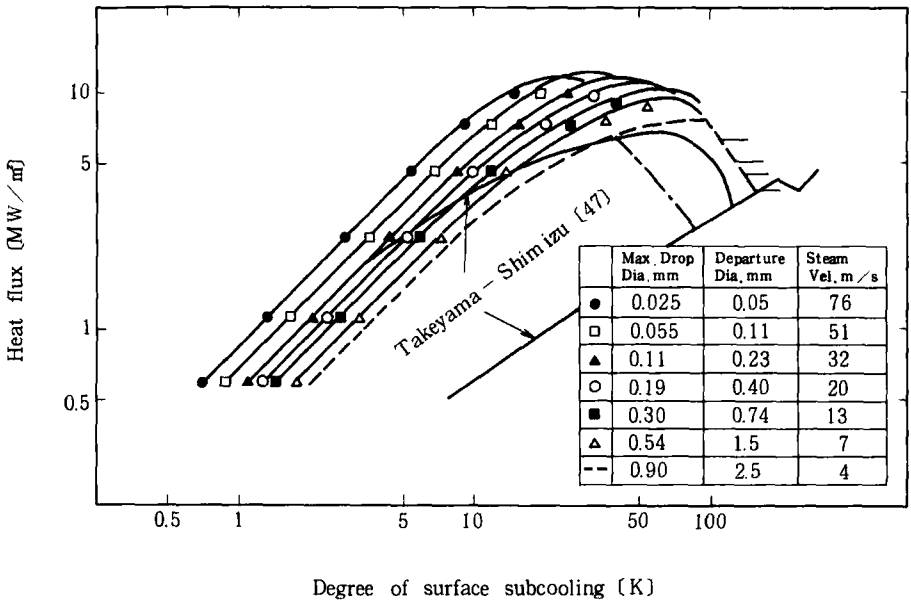

FIG. 18. Condensation curves.

suggests that the heat transfer performance on lower tubes among a vertical tube array may not be deteriorated much by impingement of liquid dripping from the upper tubes. In other words, the condensate inundation would not cause much of a problem in the case of dropwise condensation. This superposition has been verified by Tanasawa and Saito [49].

5. *Effect of Material Thermal Properties*

The surface temperature of the condensing surface was once assumed tacitly (or carelessly) to be uniform and constant when defining the heat transfer coefficient by dropwise condensation. However, because there are drops of various different sizes on the surface, and because those drops are moving randomly due to coalescence and departure, the temperature and the heat flux on the condensing surface must be nonuniform and incessantly fluctuating. As a matter of fact, such a temperature fluctuation has been observed by a number of investigators.

Fluctuation and nonuniformity of the surface temperature are inherent to the finite thermal conductivity of the surface material. Its possible effect on the heat transfer coefficient was first predicted theoretically by Mikić [50].

The thermal resistance (denoted R) between the vapor and the condensing surface must be nonuniform over the surface because drops of different sizes are distributed. Owing to that, the distribution of the heat flux on the surface must also be nonuniform. If the thermal conductivity of the surface material is finite, the local surface temperature T_c depends on the local heat flux. If the average heat flux over the entire surface is denoted as $\dot{q}$, and the corresponding surface temperature is denoted T_s, then T_c takes on a much larger value than T_s where R is smaller. On the other hand, because the mean heat flux is an average of the local heat flux, it follows that

$$\dot{q} = \frac{1}{A}\int_A \frac{T_v - T_c}{R} dA \tag{30}$$

For an ideal condensing surface having infinitely high thermal conductivity, $T_c = T_s$, and then

$$\dot{q} = (T_v - T_s)/R_0 \tag{31}$$

where

$$\frac{1}{R_0} = \frac{1}{A}\int_A \frac{1}{R} dA \tag{32}$$

For an actual surface material with finite thermal conductivity, T_c varies on the surface. If we define an average surface temperature T_{cm} as

$$T_{cm} = \frac{R_0}{A}\int_A \frac{T_c}{R} dA \tag{33}$$

then Eq. (30) can be written as

$$\dot{q} = \frac{T_v - T_{cm}}{R_0} = \frac{T_v - T_s}{R_0}\,\frac{T_v - T_{cm}}{T_v - T_s} \tag{34}$$

In the experiment, we usually measure the average heat flux $\dot{q}$ and the surface temperature T_s, and derive the heat transfer coefficient h from the following relation:

$$h = \dot{q}/(T_v - T_s) \tag{35}$$

By rewriting this equation, we get

$$\frac{1}{h} = \frac{T_v - T_s}{\dot{q}} = \frac{T_v - T_{cm}}{\dot{q}} + \frac{T_{cm} - T_s}{\dot{q}} = R_0 + R_s \tag{36}$$

This equation indicates that T_s is not equal to T_{cm} on a surface having a finite thermal conductivity, and that there exists another thermal resistance R_s on top of the resistance R_0. This thermal resistance R_s is the constriction resis-

tance, i.e.,

$$R_s = (T_{cm} - T_s)/\dot{q} \tag{37}$$

According to the Mikić theory, the heat transfer coefficient by dropwise condensation must be lower on a condensing surface made of a poor conductive material. That is to say, the heat transfer coefficient on a stainless-steel surface must be lower than that on a copper surface.

Several groups of researchers have carried out measurements to find out the effect of surface thermal conductivity on the heat transfer coefficient by dropwise condensation. Some of those results are plotted in Fig. 19. The figures shows two opposite tendencies. The results obtained by Aksan and Rose [51] (line A) make us consider that the heat transfer coefficient is substantially independent of the surface thermal properties. The results of experiments done afterward by Rose [52] and Stylianou and Rose [53] (in which the overall heat transfer rates are compared) have shown similar tendencies. On the contrary, Tanner *et al.* [54], Wilkins and Bromley [55], and Hannemann and Mikić [56] (lines B, C, and D) insist that the heat transfer coefficients on the poorly conductive materials are lower.

Regarding such a discrepancy among the results, discussion continued for nearly 20 years. However, recent papers by Tsuruta and Tanaka [57] and Tsura and Togashi [58] seem to settle the controversy. In the first place,

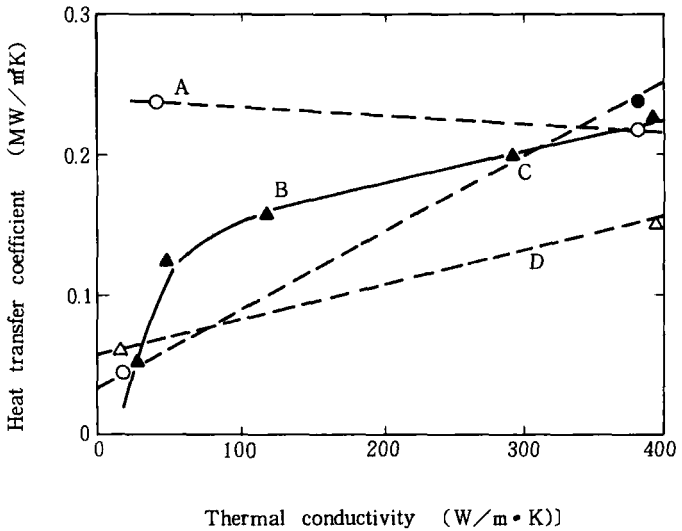

FIG. 19. Dependence of heat transfer coefficient of dropwise condensation on the thermal conductivity of surface materials. (○), Askan and Rose [51]; (△), Hannemann and Mikić [56], (●) Tanner *et al.* [54]; (▲), Wilkins and Bromley [55].

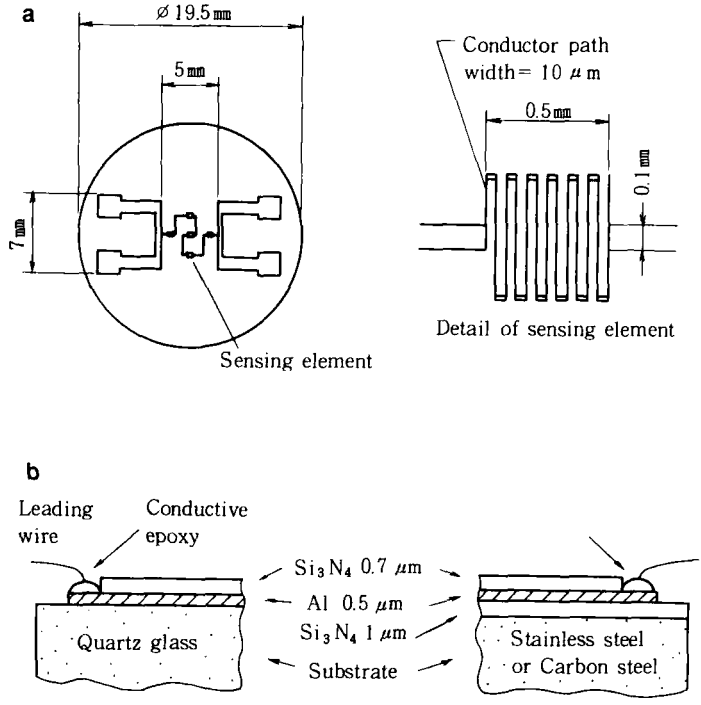

FIG. 20. Thin-film surface thermometer. (a) Pattern of aluminum resistor. (b) Make-up of thin-film thermometer.

Tsuruta and Tanaka [57] derived theoretically a differential formulation, which describes the constriction resistance as the function of the surface thermal conductivity, the maximum and minimum drop radii, and the interfacial mass transfer resistance. Following this, Tsuruta and Togashi [58] carried out an experiment to verify the theory. They used thin-film temperature sensors (Fig. 20) made of aluminum to measure the surface temperature directly and accurately. They measured the heat transfer coefficient of dropwise condensation on the surfaces of quartz glass (thermal conductivity $\lambda_c = 1.3$ W/m K), stainless steel ($\lambda_c = 16.0$ W/m K), and carbon steel ($\lambda_c = 51.6$ W/m K), under different reduced pressures of 1–10 kPa.

Shown in Fig. 21 are their experimental results, together with the theory by Tsuruta and Tanaka. Results of measurement on a copper surface by Hatamiya and Tanaka [41] are also plotted. Agreement between experiment and theory is fairly good. It shows that the heat transfer coefficient by dropwise condensation of steam on the quartz glass plate is about one-tenth that on the copper surface, when compared at a pressure of 0.1 atm.

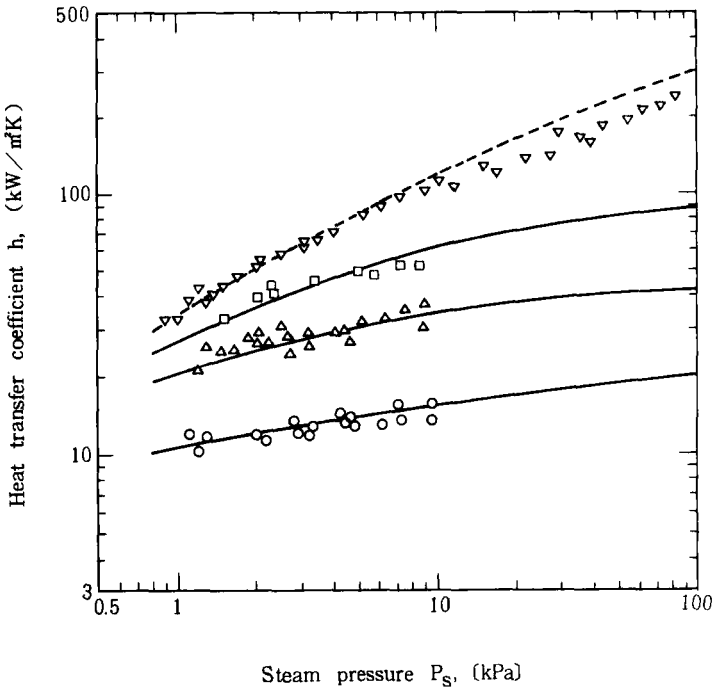

FIG. 21. Heat transfer coefficient of dropwise condensation of steam on four different surface materials. Experimental data: (○), Quartz glass; (△), stainless steel; (□), carbon steel; (△), copper. From Hatamiya and Tanaka [41].

In addition to theoretical considerations and experiments with homogeneous surfaces (which are assumed to be sufficiently thick), Tsuruta [59] has coped with a case in which a layer of poorly conductive material covers the surface of another material. Such a case is important when considering the use of coating by a hydrophobic material, e.g., poly(tetrafluoroethylene) (PTFE) as the promoter for dropwise condensation. One of the results is shown in Fig. 22. As is expected, the thicker the PTFE coating, the lower the heat transfer coefficient.

6. *Heat Transfer Coefficients Obtained under Other Conditions*

a. *Measurements on High-Pressure Steam.* Heat transfer coefficients of steam at pressures higher than 1 atm have beem reported by several investigators. However, we will not introduce them here because the reliability of those results are doubtful.

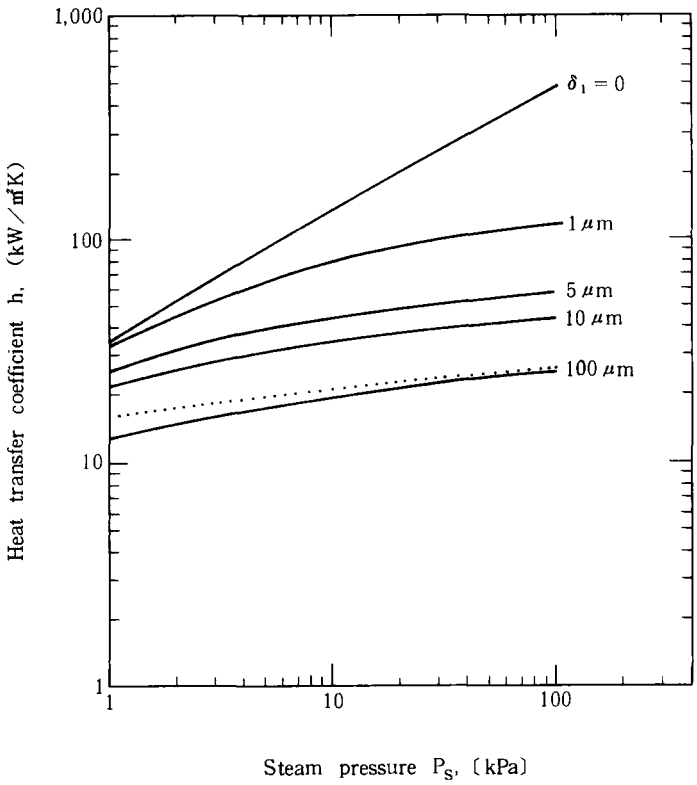

FIG. 22. Heat transfer coefficient of dropwise condensation on surfaces covered with poly(tetrafluoroethylene) film. (—), PTFE surface, r_{max} = 1.5 mm; (···), Nusselt theory, ΔT = 2 K.

b. *Dropwise Condensation at Small Vapor-to-Surface Temperature Differences.* In Section IV,B,4, the change of the heat flux along with the increase in the surface subcooling ΔT, i.e., condensation curve, is discussed. On the contrary, the phenomenon that might occur when ΔT is reduced is also of interest. At smaller ΔT, the rate of drop nucleation may be reduced because the critical radius of drop formation must be larger. Because measurements under smaller ΔT accompany technical difficulties, most of the results [33,34,60–62] reported up to now involve, more or less, some inaccuracy. More efforts will be needed in the future.

c. *Dropwise Condensation of Organic Vapors.* When considering applications to condensers to be used in chemical plants (e.g., distillation plants) and energy conversion devices (e.g., heat pumps and refrigerators), dropwise

condensation of organic vapors should be investigated extensively. However, this has not been the case, mainly because a method of surface treatment to maintain dropwise condensation has not yet been established. Up to now, experiments have been performed with vapors of ethylene glycol (ethanediol), propylene glycol, aniline, nitrobenzene, and methanol, for example. Dropwise condensation has not been observed for vapors of freons and their substitutes.

d. *Dropwise Condensation of Metal Vapors.* Reports have been published on dropwise condensation of mercury vapor. Among them, papers by Rose and colleagues [22,23,63,73,74], Kollera and Grigull [64,65], and Ivanovskii *et al.* [66] have yielded apparently reliable results. No reports have been published on dropwise condensation of other metal vapors, such as sodium, NaK, and potassium, though the liquid phases of these substances have rather large surface tensions.

It should be noted that, as discussed in Section III, the interfacial resistance to mass transfer at the liquid–vapor interface plays an important role in the condensation of metal vapors. The total resistance to condensation should be calculated using an equation similar to Eq. (21).

C. HEAT TRANSFER THEORY

The theory of heat transfer by film condensation was established by Nusselt [2] more than 75 years ago, but no complete theory has yet been proposed for dropwise condensation. This is due to the very complicated nature of the dropwise condensation phenomenon. In addition to the randomness of the local and instantaneous distribution of drop size, the locations of the drops change very frequently due to coalescence and drop detachment, resulting in fluctuation and nonuniformity of the surface temperature. Therefore, how to handle such random processes becomes the most important problem to be solved.

Of the theories of dropwise condensation proposed up to the present, only two seem to be near completion: one proposed by Le Fevre and Rose [67] and Rose [45,68,88] and one proposed by Tanaka [43,44,69–71].

1. *Le Fevre–Rose Theory*

This theory [67], first proposed in 1966 and revised afterward, attempts to derive the heat transfer rate of dropwise condensation of a pure vapor from the combination of the following two properties: (1) the heat transfer resistance of a single drop of given size, and (2) the average heat transfer coefficient on the surface, talking into consideration the drop size distribution.

Nonuniformity and fluctuation of the surface temperature are not considered in the analysis.

On deriving the heat transfer resistance of the single drop, the following three items are accounted for: (1) the influence of surface curvature on the phase equilibrium temperature, (2) the mass transfer resistance at the liquid–vapor interphase, and (3) the heat conduction resistance through the drop. (The thickness of promoter layers was involved in the original paper [67], but later its effect was neglected because it was considered small.)

The relation between the heat flux $\dot{q}_B$, which goes from the base of a hemispherical drop into the condensing surface, and the surface subcooling ΔT is expressed as

$$\Delta T = \frac{2\sigma}{r}\frac{v_l T}{h_{fg}} + \left(\frac{K_1 r}{k_l} + \frac{K_2 v_v T}{h_{fg}^2}\frac{\kappa+1}{\kappa-1}\sqrt{\frac{RT}{2\pi}}\right)\dot{q}_B \tag{38}$$

where T is the saturation temperature of the vapor, r is the drop radius, σ is the surface tension, v_l and v_v are the specific volumes of the condensate and the vapor, respectively, h_{fg} is the latent heat of condensation, k_l is the thermal conductivity of the condensate, and κ is the ratio of specific heats. The first term in the right-hand side of Eq. (38) represents the reduction of the vapor-to-surface temperature difference due to condensation on the convex liquid surface. The first term in the parentheses represents the conduction resistance of the drop with radius r, where K_1 is a constant relating the temperature drop in the drop ΔT_d to $\dot{q}_B$ and is defined as

$$\dot{q}_B = k_l(\Delta T_d / K_1 r) \tag{39}$$

This equation means that the drop with radius r is replaced by a liquid layer with uniform thickness $K_1 r$. Le Fevre and Rose assumed $K_1 = 2/3$ because a circular cylinder having an equal volume with a hemisphere is $(2/3)r$.

The second term in the parentheses comes from the interphase mass transfer resistance. Here, Le Fevre and Rose use an expression based on a result by Schrage [11] (which is introduced in Section III) for a monoatomic gas, and the condensation coefficient is taken as unity. The presence of a ratio $(\kappa+1)/(\kappa-1)$ is due to a correction for polyatomicity. This correction has a relatively small effect for steam but is important for complex molecules when κ is closer to unity. Another constant K_2 appearing here is the ratio of the base area of a drop to its curved surface area, i.e., for hemispherical drops $K_2 = 1/2$.

Thus, the right-hand side of Eq. (38) represents a series connection of temperature drops due to three different causes. To obtain the average heat transfer coefficient over a whole condensing surface, the distribution of drop size is to be considered as the next step. If the fraction of surface area covered

by drops with radii between r and R_{max} (the maximum drop radius) is denoted f, its functional form is assumed by Le Fevre and Rose as

$$f = 1 - (r/R_{max})^n \tag{40}$$

Equation (40) involves an unknown exponent, n, and has the properties that no area is covered by drops greater than the largest, and that if the distribution extended to drops having zero radius, then the whole surface would be covered.

The surface heat transfer coefficient is then given by

$$h = \frac{1}{\Delta T}\int_{R_{min}}^{R_{max}} \dot{q}_B\left(-\frac{df}{dr}\right)dr \tag{41}$$

because the fraction of surface area covered by drops having radii between r and $r + dr$ is $(-df/dr)\,dr$. If Eqs. (39) and (40) are substituted into Eq. (41), we get

$$h = \frac{n}{R_{max}^n \Delta T}\int_{R_{min}}^{R_{max}} \frac{\dfrac{\Delta T}{T} - \dfrac{2\sigma v_l}{r h_{fg}}}{\dfrac{K_1 r}{k_l T} + \dfrac{K_2 v_v}{h_{fg}^2}\dfrac{\kappa+1}{\kappa-1}\sqrt{\dfrac{RT}{2\pi}}} r^{n-1}\,dr \tag{42}$$

For the lower limit of integration, R_{min}, the radius of the smallest viable drop was taken, i.e.,

$$R_{min} = \frac{2\sigma v_v}{h_{fg}}\frac{T}{\Delta T} \tag{43}$$

On the other hand, the maximum drop radius, R_{max}, was obtained from the dimensional analysis as follows:

$$R_{max} = K_3\sqrt{\frac{\sigma}{(\rho_l - \rho_v)g}} \tag{44}$$

In most of the cases ρ_v is much smaller than ρ_l and can be omitted. Equation (44) involves another constant K_3, and Le Fevre and Rose assumed $K_3 \approx 0.4$ for dropwise condensation of steam on vertical plates. Substituting the values of σ, ρ_l, g, and K_3 ($=0.4$) into Eq. (44) we get $R_{max} = 1.0$ mm.

To calculate the integral in Eq. (42), the value of the index n must be determined. Le Fevre and Rose evaluated Eq. (42) for various values of n and found that excellent agreement was obtained, as may be seen from Fig. 23, between experiments and the theory if n was assigned a value of 1/3. Afterward, the theory was compared favorably with data for low-pressure steam [39,53], using the constants given above. Also, the theory was compared with data for ethylene glycol at various pressures [72] and with data for mercury

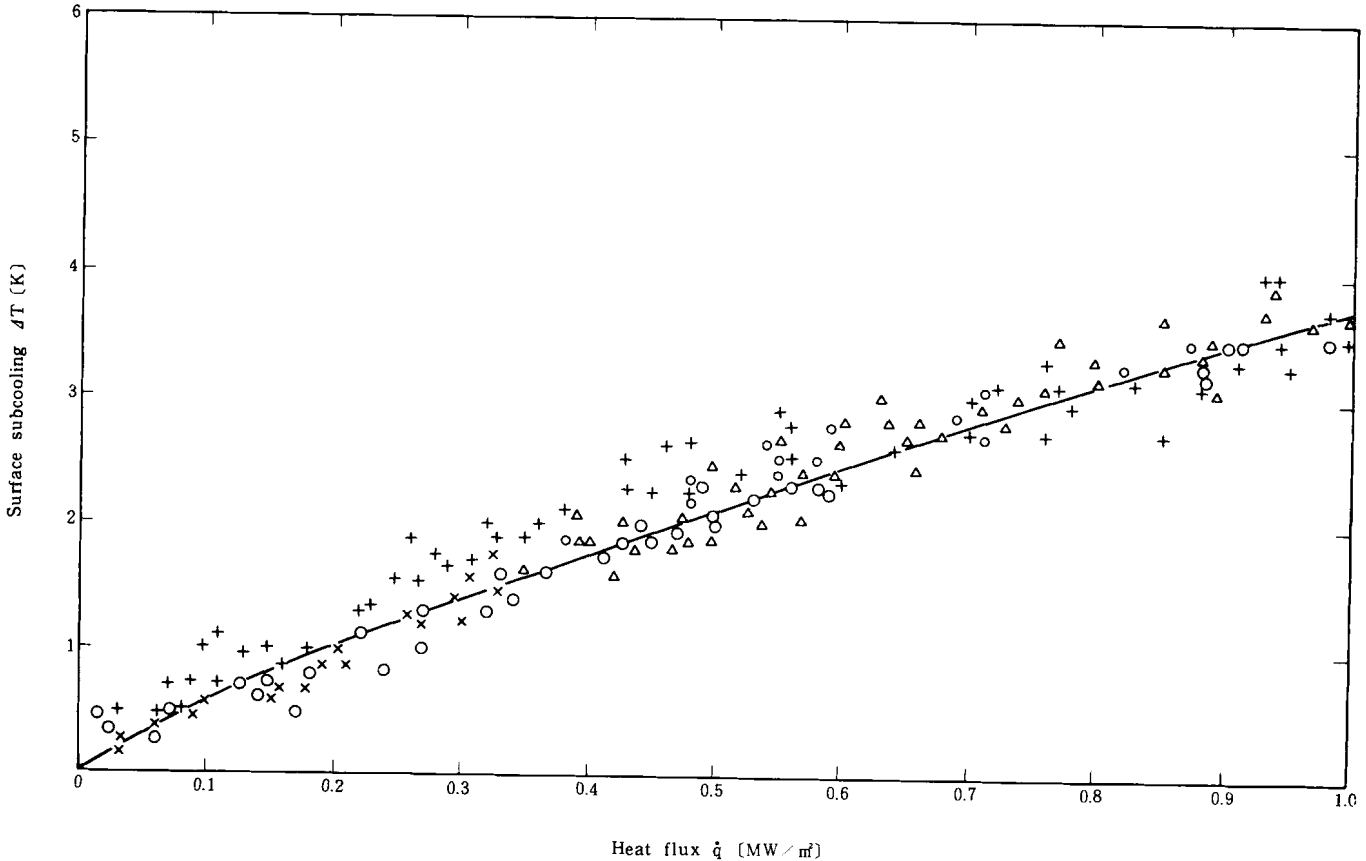

FIG. 23. Comparison of Le Fevre–Rose theory with experimental results. (—), Le Fevre and Rose [67]; (○), Le Fevre and Rose, [35, 36]; (○), Tanner *et al.* [33]; (+), Citakoglu and Rose [37]; (x), Graham [34]; (△), Wimshurst and Rose [39].

on stainless steel [73,74]. However, in those cases the constants used had to be somewhat different from those employed for steam at 1 atm in order to get good agreement between the theory and the experiment.

It is interesting to note that the value of the index, $n = 1/3$, leads to a relation showing that the heat transfer coefficient of dropwise condensation is approximately proportional to $R_{\max}^{-1/3}$. This relation is very close to the experimental result obtained by Tanasawa *et al.* [42] (Fig. 16).

Another interesting thing is the drop size distribution. If the number of drops having a radius between r and $r + dr$ is denoted $N(r)\,dr$, it is related to f defined by Eq. (40) as follows:

$$f = \int_r^{R_{\max}} Ar^2 N(r)\,dr \tag{45}$$

or

$$N(r) = -\frac{1}{Ar^2}\frac{df}{dr} = \frac{1}{AR_{\max}^n} r^{n-3} \tag{46}$$

where A represents the ratio of the base area of the drop to the radius (of curvature) squared, and when the drop is a perfect hemisphere, then $A = \pi$. If the value of $n = 1/3$, which is adopted by Le Fevre and Rose, is used, Eq. (46) suggests that the drop size distribution function is proportional to r to the power $-8/3$.

On the other hand, the distribution of the drop radius has been measured by several researchers (e.g., Graham [34] and Tanasawa and Ochiai [75]). According to Tanasawa and Ochiai, the function $N(r)$ is expressed as follows:

$$N(r) = 0.159r^{-2.54}, \qquad 0.005 \le r < 0.25 \tag{47a}$$

$$N(r) = 0.0316r^{-3.87}, \qquad 0.25 \le r < 0.96 \tag{47b}$$

where r is expressed in millimeters. It should be noted that the exponent to r, -2.54, in Eq. (47a) is very close to $-8/3$. Compared in Fig. 24 are the drop size distributions obtained by experiments [34,75], by numerical simulations [76] (which are not mentioned here), and by theory [67,77]. All of these agree quite well. In addition, a similar result has been obtained by Tanaka [69–71], which is to be introduced later. This might suggest that the distribution of the drop size is determined almost uniquely, irrespective of the randomness of the process of drop formation or coalescence.

2. *Tanaka's Theory*

A theory proposed by Tanaka [43,44,69–71] in 1973 and 1974 is the most elaborate and sophisticated in coping with the mechanism of dropwise

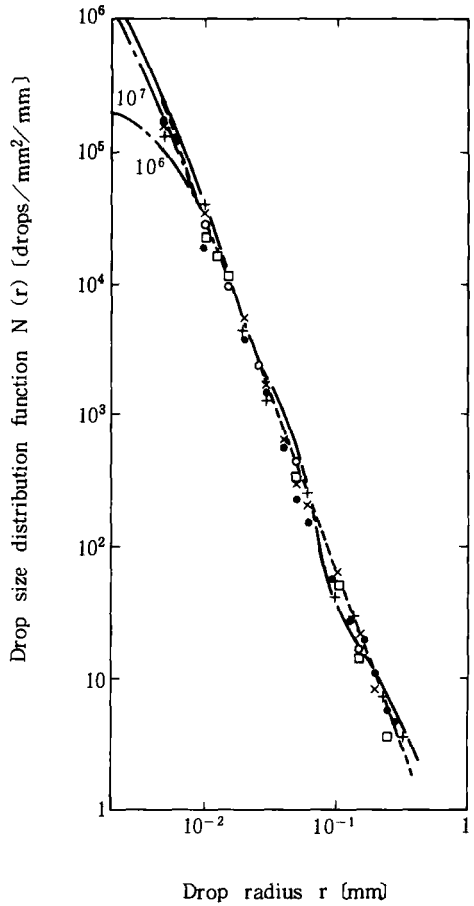

FIG. 24. Drop size distribution. (—), Rose and Glicksman [77]; (----), Le Fevre and Rose [67]; (– – –), Glicksman and Hunt [76]. (Figures represent site densities per cm^2.) (○, □), Graham [34]; (●, +, ×), Tanasawa and Ochiai [75].

condensation. The theory considers the transient change of local drop size distribution, taking into account the processes of growth and coalescence of drops. In the following discussion, only an outline of Tanaka's theory is introduced. For more detail the original papers should be referred to.

Let us denote the number of drops per unit area having radii between r and $r + dr$ as $N(r, t)\,dr$. Here, t is the time elapsed after the area of the condensing surface of interest was swept off by a departing drop. One of the important features of Tanaka's theory is that it focuses attention on the transient growth

and coalescence process of drop behavior. The drops formed on the bare surface grow by direct condensation (see Fig. 3) with a rate of $\dot{r}_e(r)$, but, because coalescence between drops takes place at the same time, the apparent rate of growth is, as an average, $\dot{r}_a(r,t)$.

In such a situation, the relation below is derived for drops with radius r by considering the balance between growth and loss (by coalescence and sweep).

$$\frac{\partial N}{\partial t} = -\frac{\partial(N\dot{r}_a)}{\partial t} - \int_r^{R_{max}} 2\pi\rho\{\dot{r}_a(r) + \dot{r}_a(\rho)\}\Psi(r;N)\,N(r)\,N(\rho)\,d\rho + \pi R_{max}^2\,N(R_{max})\,\dot{r}_a(R_{max})\,N(r) \tag{48}$$

$$\Psi(r,t;N) = \frac{1}{\left(1 - \int_r^{R_{max}} \pi p^2\,N(p,t)\,dp\right)\left(1 - \dfrac{r}{r_E(r,t)}\right)} \tag{49}$$

$$r_E(r,t) = 2\frac{1 - \int_r^{R_{max}} \pi p^2\,N(p,t)\,dp}{\int_r^{R_{max}} 2\pi p\,N(p,t)\,dp} \tag{50}$$

In these equations, the product $N(r,t)\dot{r}_a(r,t)$ represents the "flux" of the number of drops per unit area and unit time that grow exceeding the radius r. Then the first term in the right-hand side of Eq. (48) signifies the difference between the "afflux" from drops smaller than r and the "efflux" into drops larger than r. The second term in the right-hand side of Eq. (48) represents the number of drops lost by coalescence, and subtraction of this number from the first term is equilibrated with the left-hand side, which is the rate of increase of the number of drops. The third term is for correction of the reduction of the area to be considered due to the departure of drops. Further, the function $\Psi(r,t;N)$ is necessary to take into account the requirement that every drop does not overlap each other. The variable r_E defined by Eq. (50) is the "equivalent diameter for clearance" and is the area that is not covered by drops divided by the sum of the peripheral length of the drops. It is a measure of how closely packed the drops are.

The equation as follows is derived for the volume increase of a drop with radius r when the drop grows by coalescence:

$$\int_{R_{min}}^{r} \frac{2}{3}\pi\rho^3 2\pi r[\dot{r}_a(r) + \dot{r}_a(\rho)]\Psi(\rho;N)\,N(\rho)\,d\rho = 2\pi r^2(\dot{r}_a - \dot{r}_e) \tag{51}$$

where it is assumed that the drops are hemispheric. The left-hand side of Eq. (51) gives the volume increase due to coalescence and the right-hand side is

the difference between the volume increase by apparent growth and the increase by the growth due to direct condensation.

If $\dot{r}_e(r)$ is known and the initial drop size distribution $N(r, 0)$ is given, and, further, if one more restrictive condition is settled, then the set of Eqs. (48) and (51) can be solved to yield $N(r, t)$ and $\dot{r}_a(r, t)$. Here, Tanaka adopted the rate of drop growth obtained by Fatika and Katz [78] as for $\dot{r}_e$, and assumed as a restrictive condition that the equivalent diameter for clearance is equal to the average minimum distance between nucleation sites, D, i.e.,

$$r_E(R_{min}, t) = D \tag{52}$$

and solved Eqs. (48) and (51) numerically. Figure 25 shows an example of the result, where $T_v = 100°C$, $\Delta T = 1°C$, $R_{max} = 1.0$ mm, $R_{min} = 0.006$ mm, and

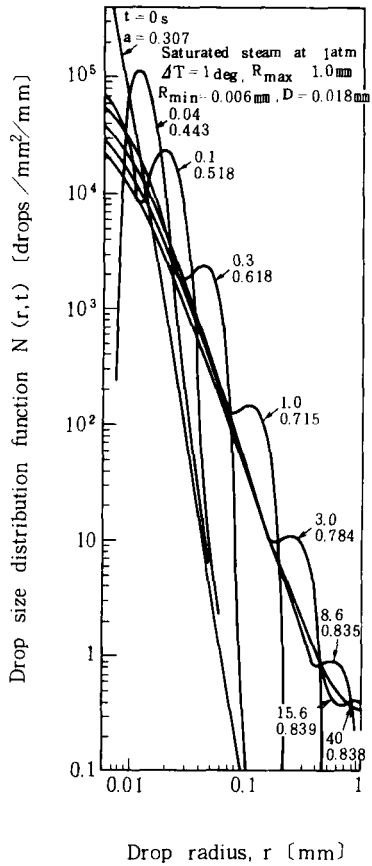

FIG. 25. Timewise change of drop size distribution.

$D = 0.018$ mm. Shown in the figure is a change of the drop size distribution from $t = 0$ to $t = 40$ sec. A main feature of this result is the fact that the drop size distribution at every instant has a small "hill" near the right end of the curve, and the hill moves down to the right as the time proceeds. The shape of the curve becomes similar after $t = 0.3$ sec, and simply moves along the straight line with a gradient of -3. On the other hand, the drop size distribution to the left of the hill is approximated by a straight line, of which the gradient is -2.68, if the fraction of area covered by all the drops is assumed unity. This value of -2.68 almost coincides with that in Eq. (47a) and also with one obtained by Le Fevre and Rose, i.e., $-8/3$. It should be added here that the distribution function, $N(r)$, which appeared earlier, is the average of $N(r, t)$ with respect to time and area.

Furthermore, Tanaka derived the heat transfer coefficient using $\dot{r}_a(r, t)$ and $N(r, t)$ obtained from Eqs. (48) and (51), and derived the following relation:

$$hR_{max}/k_l = 5.3(R_{max}/D)^{0.7} \tag{53}$$

where k_l is the thermal conductivity of the condensate. Equation (53) shows that the heat transfer coefficient is proportional to R_{max} to the power -0.3, which agrees well with the experimental result by Tanasawa *et al.* [42] and with the theory by Rose [45], both of which are introduced in Section IV,B,3.

There are a few doubtful points in Tanaka's theory. For instance, the theory employs as the rate of drop growth the result by Fatika and Katz [78], which is now proved to be incorrect. At the same time, the fluctuation of local surface temperature is not considered, and the way of using the distance between nucleation sites, D, is questionable. In spite of all of these discrepancies, this theory seems to describe the process of dropwise condensation most accurately.

D. Methods of Maintaining Dropwise Condensation for a Long Period of Time

Although there remain quite a few yet-unsolved problems on dropwise condensation, there is little doubt that the heat transfer coefficient of dropwise condensation is remarkably high. If the presupposition of film condensation, which the design procedures of most of condensers are usually based on, could be changed to that of dropwise condensation, a substantial economy of materials, dimensions, and, possibly, costs might be achieved. Of course, it is solely the vapor-side heat transfer that is improved by dropwise condensation, because the overall heat transfer is dependent also upon the thermal resistance of the solid wall and the coolant-side heat transfer. And still, a rough estimation reveals that if dropwise condensation is available on the vapor side, the overall heat transfer coefficient is doubled and hence the heat transfer

surface area is reduced to half, in the case of water vapor. This will result in a considerable reduction of the cost of a condenser.

An objection that might be raised here most commonly may be that the vapor-side thermal resistance can be reduced without employing dropwise condensation. As a matter of fact, and as will be dicussed later, the so-called high-performance condensing surfaces of a variety of types have been developed in recent years. Among them are microstructured surfaces that make use of the effect of the capillary force on top of the effect of extended area. These high-performance condensing surfaces have indeed considerably small vapor-side heat transfer resistance at their optimum operating condition. However, such an excellent performance is usually limited to a relatively narrow range of operating conditions. Especially, at higher condensing rate, cavities on the microstructured surface are flooded with condensate and the capillary force becomes ineffective. In addition, fouling by various causes may easily deteriorate the high performance.

On the other hand, in the case of dropwise condensation, a very high heat transfer rate is available even at a very high heat flux. In addition to this, there is a possibility that the low-energy surface for dropwise condensation can be manufactured less expensively, if an excellent technique for surface treatment is developed in the future. In reality, however, to find out techniques most effective in promoting dropwise condensation for a sufficiently long period of time is the most important and serious problem to be solved before the practical application of dropwise condensation ceases to be a mere dream.

The methods (both on a laboratory scale and an industrial scale) employed up to present to maintain dropwise condensation are classified into the following five categories:

1. Application of an appropriate nonwetting agent, i.e., organic promoter, to the condenser surface before operation.
2. Injection of the nonwetting agent intermittently (or continuously) into the vapor.
3. Coating the condensing surface with a thin layer of an inorganic compound such as metal sulfide.
4. Plating the condensing surface with a thin layer of a noble metal such as gold.
5. Coating the condensing surface with a thin layer of an organic polymer such as poly(tetrafluoroethylene) (PTFE).

The first method has been used most commonly to obtain dropwise condensation in laboratory apparatus. A solution of organic promoter may be wiped, brushed, or painted on the surface, or it can be sprayed directly on the surface. Sometimes the surface is immersed into a solution of promoter. In every case the promoter chemisorbs on the substrate in question. It seems

there is little evidence indicating that one method is more effective than another. The adsorbed layer thus obtained is proved to be nonwetting as long as it is thicker than a few molecular layers. Hence, the amount of promoter needed to produce dropwise condensation is very minute. What matters is how long such a surface can sustain dropwise condensation. Tests have been carried out for a number of such substances. The most systematic study among them has been done by Blackman *et al.* [79]. They discussed in detail the necessary characteristics that the promoters should possess and synthesized 37 compounds that would serve the purpose. Condensation tests were performed for all these compounds and it was proved that a compound called glycerol tri-[11-ethoxy(thiocarbonyl)thiundecanoate] exhibited the longest lifetime; perfect dropwise condensation was observed for 3530 hr (about 21 weeks). This is a very encouraging report and we are inclined to believe that when an adequate promoter is chosen to be applied to a carefully cleaned surface, dropwise condensation lasts for a sufficiently long period. But this may happen only in the most ideal case in which every condition is kept satisfactory. The same may not be expected in industrial systems, for degradation of promoter due to impurities deposited out of the vapor and stripping off by some mechanical causes are very likely.

The second method, namely, periodic (or continuous) injection of promoter into the vapor, could be a useful technique, because the stripped-off promoter layer will be replenished at once. Blackman *et al.* [79] have reported that the minimum amount of promoter needed for injection method is about 0.02–0.1% of the vapor, though it depends on the substrate and the promoter. This amount will not matter economically, if some fraction of it is recovered afterward. Problems with the injection method are possible contamination and corrosion of the surface. However, once these problems are solved, this method seems more promising than the first.

Erb and Thelen [80] have published the result of their systematic tests on the third method. They have paid attention to the fact that sulfides of copper and silver exhibit extremely low solubility in water. The hydrophobic nature of these mineral sulfides has also been known. Tests were done for a number of sulfided metal surfaces. Among them, a sample of sulfided silver on mild steel showed excellent dropwise condensation after more than 10,000 hr (about 60 weeks) of exposure to continuous condensation.

Although this result seems very promising, there are a couple of things that are not clear. In the first place, the reproducibility of their test results seems not so good. Considerably different lifetimes have been observed for the same surfaces with similar treatments. Second, the authors did not give a strong recommendation to the use of sulfided surfaces for dropwise condensation. Instead, they recommended the use of noble metal-coated surfaces as described below. It is not obvious if this is owing to the expenses involved in sulfiding the metal surfaces or owing to other reasons.

In the condensation study mentioned above, Erb and Thelen [80] found that the unsulfided silver surface had even better dropwise condensation than the sulfided silver sample. By comparison of the position in the periodic table (Cu–Ag–Au), they predicted that gold also would produce dropwise condensation.

That some noble metal-plated surfaces, especially gold-plated surfaces, produce dropwise condensation had been known from experience by quite a few researchers. Experiments have been carried out using gold-plated condenser surfaces without any organic promoter. Extensive condensation studies were made by Erb and Thelen [80] on silver, gold, rhodium, palladium, chromium, and platinum surfaces. Three of these surfaces (gold, palladium, and rhodium) exhibited good dropwise condensation for more than 12,500 hr (1.43 years). It was found that, of the three, gold was the most reliable because it was not adversely affected by a period of shutdown in air as the other two sometimes were for a period of time.

A question has been raised, however, whether the gold surface possesses genuine nonwettability. Wilkins *et al.* [81] have reported that the steam condenses as a film on a very carefully cleaned gold surface. They have concluded that, in Erb and Thelen's experiment, some organic compounds adsorbed onto the gold surface must have promoted dropwise condensation. Against this, Erb [82] has insisted that a thin oxide layer was formed on the gold surface in the case of Wilkins and others' experiment and it rendered the surface wettable.

A definite conclusion to this debate has not yet been reached. However, judging from results of recent works (e.g., Refs. [83,84]), it seems that uncontaminated surfaces of noble metals always result in filmwise condensation. However, electroplated gold (and silver, too) surfaces are powerful adsorbers of trace organic materials from the surroundings and the absorbed organics cause dropwise condensation. But considering practical use, it does not matter whether some impurities are adsorbed on the surface. Of greatest significance is whether the surface can really produce long-term dropwise condensation. In this respect, the work by Erb and Thelen should be appreciated. Another important thing to be considered is the economical feasibility. Erb and Thelen have compared by a simple analysis the surface coating cost with the overall condensation cost savings due to gold plating for the case of a distillation plant for saline water conversion. They have reached the conclusion that the gold-plating approach to dropwise condensation is economically feasible, provided that the coating cost is reduced to some extent. As a countermeasure they have proposed what they call low-cost multilayer systems. Nevertheless, it seems still too early to have an optimistic outlook before technical problems are thoroughly solved.

Seemingly, many people consider that the fifth method, i.e., polymer coating, is more promising. Since World War II a great number of highly

polymerized compounds having various physical and chemical properties have been manufactured. Some of them have very low surface energies and cannot be wetted by liquids such as water. The most typical of them is poly(tetrafluoroethylene) (PTFE, or Teflon). Attempts have been made to produce long-term dropwise condensation using PTFE-coated surfaces.

A couple of difficulties have to be overcome before the polymer film approach to the industrial use of dropwise condensation attains success. The first is to form a film with good adhesion to the substrate, few voids, and sufficiently high mechanical strength. The second is to make the film thin enough not to excessively retard heat transfer with its low thermal conductivity. Because the thermal conductivity of a polymer such as PTFE is as low as 0.25 W/m K, the allowable maximum thickness of the film may be the order of 1 μm, taking into account both the conduction and the constriction resistances (see Section IV,B,5). These two difficulties are related each other, and a solution to the one (for example, thinning the film) results in enhancing the other (reducing the mechanical strength). However, several new processes of forming very thin polymer coatings on the surface have been developed recently: Two examples of those are the glow–discharge method and the electrophoresis method, in both of which polymers are formed by polymerization directly on the substrate from monomers. At any rate, the use of polymer coatings to promote dropwise condensation seems to have the advantage of lower cost when compared with the noble metal-plating method.

A little more than 10 years ago, the present author considered that the most promising of the five methods described above was the use of polymer coating, the next being the injection method. The author's opinion has changed a little. Now the author believes that the best way is to use a metal coating, not necessarily of noble metals, but of metals such as chromium. Although there is no firm theoretical basis that can explain why some metal coatings promote dropwise condensation for a considerably long period, no one can deny the fact that dropwise condensation can be maintained long enough on such surfaces. In the not so distant future a theoretical explanation will catch up with the fact.

V. Film Condensation

A. INTRODUCTION

As stated in the beginning of Section III, the theory of heat transfer by film condensation on plane and horizontal cylindrical surfaces was established first by Nusselt [2] in 1916, more than 70 years ago. The theory is useful even today. In the world of engineering, which is continually developing, it is very seldom

that a theory proposed more than 70 years ago is still effective. The Nusselt theory is one of such a rare example. Its long-standing effectiveness means that the theory grasps the very essential nature of film condensation. However, the Nusselt theory was founded on many idealizations in the modeling of the actual phenomena. Whenever the assumptions for idealization fail, modification to the theory is more or less necessary. Some of such modifications are mentioned in Section III. The other improvements are only briefly reviewed in the following discussion, focusing attention mainly on laminar film condensation outside a horizontal tube. Turbulent film, or wavy condensation, and condensation on a tube bundle are not discussed.

B. FILM CONDENSATION OF A SINGLE COMPONENT VAPOR

Among the assumptions on which the Nusselt theory is based, the one that may have a considerable effect in industrial condensers is that the vapor shear force acting on the condensate surface is neglected. Considering the vapor velocity in most condensers, the effect of the vapor shear force on condensate film thickness should be examined. Fundamentals of film condensation, including this problem, are described in textbooks (e.g., Rohsenow and Choi [85]). Reviews by Fujii and Uehara [86] and Rose [87,88] are also very instructive.

Different from the single-phase flow, the vapor flow with condensation around a horizontal circular tube is influenced both by the flow of the condensed liquid and by the suction of vapor at the vapor–liquid interface. Fujii and Honda [89] have evaluated the shear force at the interface using an approximate solution for the boundary layer, examined theoretically the effects of the vapor velocity and the thermal boundary conditions upon the heat transfer rate, and compared the result with experiment (Fujii *et al.* [90]). They found that the experimental result agreed fairly well with the theory, assuming uniform heat flux on the wall, but that the azimuthal distribution of the wall temperature differed considerably at the point of separation of vapor flow and near the location where the flows of condensate merged. They estimated that it was because they neglected the effect of heat conduction in the wall.

The correlation for the heat transfer coefficient that the authors have proposed for laminar film condensation of steam is as follows:

$$\mathrm{Nu_m}/\sqrt{\mathrm{Re_L}} = 0.96(\mathrm{Pr_L}/\mathrm{Fr}\,\mathrm{H_m})^{0.2} \qquad \text{for} \quad 0.03 \le \mathrm{Pr_L}/\mathrm{Fr}\,\mathrm{H_m} < 600 \tag{54}$$

$$\mathrm{Nu_m} = 0.69(\mathrm{Ga}\,\mathrm{Pr_L}/\mathrm{H_m})^{0.25} \qquad \text{for} \quad 600 < \mathrm{Pr_L}/\mathrm{Fr}\,\mathrm{H_m} \tag{55}$$

where $\mathrm{Nu_m}$ is the average Nusselt number ($=h_m d_o/\lambda_L$), $\mathrm{Pr_L}$ is the Prandtl number of the liquid, $\mathrm{Re_L}$ is the two-phase Reynolds number ($=U_\infty d_o/V_L$), Fr

is the Froude number ($=U_\infty 2/gd_o$), H_m is the average phase change number ($=C_{PL}\Delta T/L$), Ga is the Galileo number ($=gd_o 3/\nu_L^2$), C_{PL} is the specific heat of the liquid, d_o is the outer diameter of the circular tube, g is the acceleration of gravity, L is the latent heat of condensation, U_∞ is the approaching velocity of steam, h_m is the average heat transfer coefficient, ν_L is the kinematic viscosity of the liquid, λ_L is the thermal conductivity of the liquid, and ΔT is the area-averaged subcooling of the condensing surface.

As is well known, the Nusselt theory for natural convection film condensation on the horizontal tube with uniform wall temperature gives, in nondimensional form,

$$\mathrm{Nu}_m = 0.728(\mathrm{Ga}\ \mathrm{Pr}_L/\mathrm{H}_m)^{0.25} \tag{56}$$

The only difference between Eq. (55), which is for a low steam velocity region, and Eq. (56) is in the value of the constant on the right-hand side. And the difference is only about 5%.

After this, Honda and Fujii [91] have carried out an analysis taking into consideration the heat conduction through the tube wall. They have confirmed that the heat transfer by condensation is affected not only by the condition of steam but also by the size and the material of the tube and by the condition of cooling inside the tube. However, the effects of size, material, and cooling condition may be negligible in the case of condensation of steam, because the steam-side coefficient of heat transfer is usually much higher than the heat transfer coefficient of the coolant side. On the other hand, in the case of condensation of refrigerants like freons, the vapor-side heat transfer coefficient is rather lower than that of the coolant side. It may bring about a different situation.

Fujii *et al.* [92] have applied the result of their preceding analysis (Honda and Fujii [91]) to condensation of freon vapors and compared the result with the result of an experiment using R113 vapor. They have found that the heat transfer coefficient by film condensation of freon vapor approaches the solution for the uniform wall temperature, while that of steam shows the characteristic close to the uniform wall heat flux solution. The formula for the average Nusselt number that the authors have proposed is as follows:

$$\begin{aligned}\mathrm{Nu}_m/\sqrt{\mathrm{Re}} = {} & 0.73(\mathrm{Pr}_L/\mathrm{FrH}_m)^{0.25} \\ & \times [1 + 2.6(1 + \mathrm{Pr}_L/R\mathrm{H}_m)^{0.3}(\mathrm{Pr}_L/\mathrm{FrH}_m)^{-0.45}]^{0.3} \\ & \text{for} \quad 0.03 \le \mathrm{Pr}_L/\mathrm{FrH}_m\end{aligned} \tag{57}$$

where R is the so-called $\rho\mu$ ratio ($=\sqrt{\rho_L\mu_L/\rho\mu}$), i.e., the square root of the ratio of the product of the density and the viscosity between the liquid and the vapor. The other nomenclature is the same as those in Eqs. (54) and (55).

The right-hand side of Eq. (57) approaches that of the Nusselt equation [Eq. (56)] as the variable $Pr_L/(FrH_m)$ increases. According to the authors, Eq. (57) gives values a little higher than predicted by the experimental results for R22 by Gogonin and Dorokhov [93], but gives a little lower values than those of their own experiment for R113 vapor. However, agreement in general seems fairly good.

C. FILM CONDENSATION OF A MULTICOMPONENT VAPOR

Until recently, not much work has been accomplished on the film condensation of a multicomponent vapor consisting of more than three components. Most of the work has coped with the condensation of a two-component vapor. Condensation of a two-component vapor is classified into two categories. One is the case wherein one of the two components is a noncondensable gas, and the other is the case wherein both components condense. However, such a classification is relative to the degree of cooling, because any vapor can be condensed at a sufficiently low temperature.

Condensation of a two-component vapor, one component of which is a noncondensable gas, which is in many instances air, has been studied for the purpose of predicting deterioration of the heat transfer performance of condensers used in power plants. Because such condensers are operated at a pressure lower than 1 atm, air from outside is likely to leak inside the devices. However, recently the methodology of theoretical analysis was established and accurate and reliable results of numerical computation are available.

Figure 26 illustrates how a noncondensable gas acts to reduce the heat transfer rate of film condensation. In the case of condensation of a pure saturated vapor, the vapor pressure, P_v (which is identical with the saturation pressure, P_s), is equal to the total pressure of the gas phase, P. The temperature of the vapor is the saturation temperature, T_s, corresponding to the vapor pressure. Vapor-to-liquid phase change occurs at this temperature, provided that the interfacial mass transfer resistance discussed in Section III is negligible.

Let us assume, then, some amount of noncondensable gas is contained in the vapor. The total pressure of the gas phase is a sum of the partial pressure of vapor, P_v, and the partial pressure of a noncondensable gas, P_g, i.e., $P = P_v + P_g$. When the vapor containing a noncondensable gas touches a cold surface, only the vapor condenses and the noncondensable gas remains there. When a steady state is reached, distributions of partial pressures of both the vapor and the noncondensable gas are established as shown in Fig. 26 by dashed lines. The partial pressure of the noncondensable gas is highest at the liquid–vapor interface and decreases toward the bulk of vapor–gas mixture. On the contrary, the partial pressure of the vapor is lowest at the liquid surface. The vapor condenses at the saturation temperature corresponding to

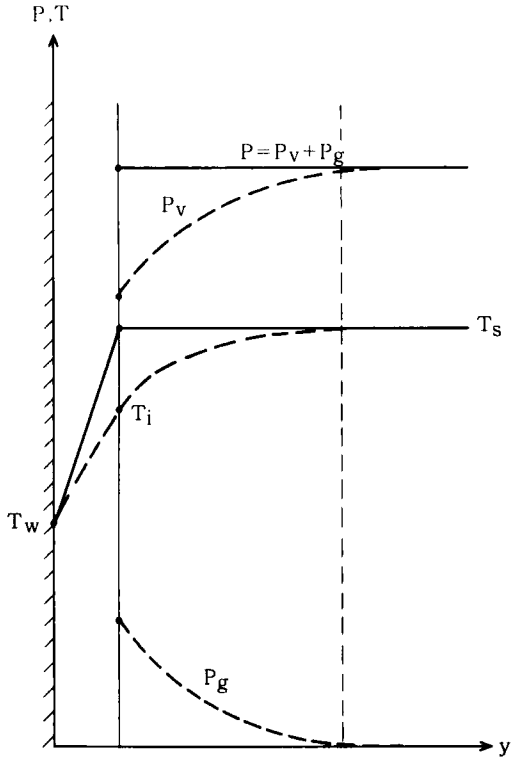

FIG. 26. Effect of noncondensable gas on condensation heat transfer.

the partial vapor pressure at the surface. This interface temperature, denoted T_i in Fig. 26, is more or less lower than T_s. The driving force for heat transfer across the condensate film decreases from $T_s - T_w$ to $T_i - T_w$. It results in a reduction of the condensing rate. The important thing here is the fact that the partial pressure of the noncondensable gas at the liquid–vapor interface (not the partial pressure in the bulk) decides the interface temperature T_i. Even if the concentration of the noncondensable gas in the bulk vapor is very small, the gas accumulates on the condensate surface when the rate of condensation is high. In order to know the value of P_g at the liquid–vapor interface, the mass transport process in the binary mixture must be analyzed. Because such an analysis is rather complicated, only a brief and simple description is given here.

Usually the heat transfer coefficient of condensation, h, is defined using the difference between the saturation temperature of vapor T_s and the surface temperature of solid T_w. If we use the temperature of the bulk vapor–gas

mixture, T_∞, in place of T_s, to define the heat transfer coefficient, we can write the following relations, which are similar to Eq. (21):

$$1/h = 1/h_g + 1/h_f \tag{58}$$

$$h_g = \dot{q}/(T_\infty - T_i) \tag{59}$$

$$h_f = \dot{q}/(T_i - T_w) \tag{60}$$

Equation (58) indicates that the overall resistance to heat transfer is a series connection of the two resistances: the one in the concentration boundary layer and the other in the liquid film. In the case of pure vapor, the former equals zero because $T_\infty = T_i$. If we denote the heat transfer coefficient of condensation of pure vapor by h_o, the ratio h/h_o represents the degree of degradation of condensation heat transfer due to noncondensable gas. To obtain this ratio, the mass transfer resistance in the concentration boundary layer, within which the partial pressure of vapor decreases, and the interfacial temperature, T_i, must be known. A very complicated task is needed for doing this, because transports of momentum, heat, and mass are coupled together.

A number of papers have been published regarding this problem. For example, Minkowycz and Sparrow [94] employed a local similarity solution to obtain effects of the variation of physical properties, the condensation coefficient, vapor superheat, thermal diffusion, and diffusion thermos. Rose [95] derived an approximate solution using the Kármán–Pohlhausen method.

Shown in Fig. 27 is a comparison of the result obtained by Minkowycz and Sparrow [94] with the results of measurement by Slegers and Seban [96] for laminar film condensation of a steam–air mixture on a vertical flat plate. Taken on the horizontal axis is the mass concentration of noncondensable gas in the bulk mixture. Although many of the experimental data are a little lower in value than the analytical results, agreement in general is not so bad. It should be noted that the heat transfer coefficient is reduced to 20–35% of that of the condensation of pure vapor, even when the bulk concentration of air is 1%.

Mori and Hijikata [97] considered that formation of mist in the concentration boundary layer would take place as the first step, and analyzed the transport process in the boundary layer, which contained minute droplets, using the Kármán–Pohlhausen method. Their result has revealed that those preceding solutions that did not take into consideration the formation of mist give reasonable results if the bulk concentration of air is not large.

Recently, the use of a large-scale computer has enabled us to obtain a more rigorous solution to this problem (e.g., Fujii and Kato [98] and Hijikata *et al.* [99]). Although details are not mentioned here, it should be noted that formulas for condensation of a binary vapor, recommended by Fujii and Kato [98] (which will be shown later), is applicable also to vapor–air mixtures.

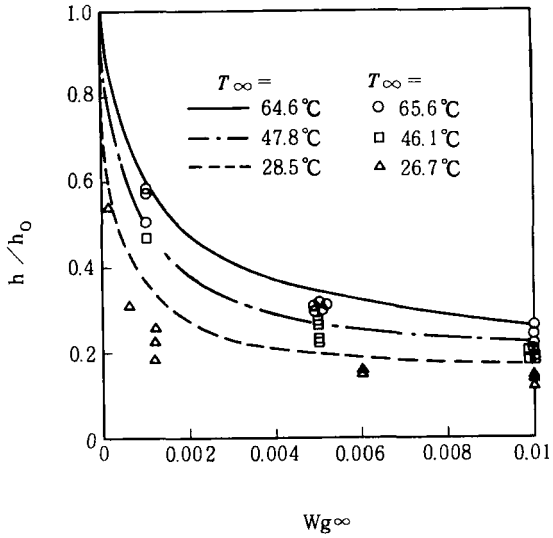

FIG. 27. Comparison of Minkowycz–Sparrow theory with experimental results. From Minkowycz and Sparrow [94]; Slegers and Seban [96].

Practical research has been performed on film condensation of a multicomponent vapor, which contains more than two condensable gases, in connection with the distillation process in chemical engineering industries. A more recent trend is that the two-component fluid has been used as the working substance in heat pump or refrigeration systems, thus stimulating research and development of the phase-change heat transfer of such a fluid. That is to say, when a pure substance is used as a working fluid for a heat pump or refrigerator, evaporation and condensation take place almost at constant temperatures, making the temperature differences at the inlets and outlets of the heat exchangers different (see Fig. 28). Because a minimum temperature difference (the so-called pinch-point temperature difference) of a few degrees is required for heat exchange, most of the heat exchange process is to be performed at larger temperature differences. The larger the temperature difference for heat transfer, the larger the irreversibility of the process, thus resulting in larger loss of the available energy.

Such a loss can be reduced by the use of a nonazeotropic multicomponent substance. When a mixture of a two-component vapor is condensed, the mixture is called azeotropic if the condensate has exactly the same molar concentration ratio as the vapor phase. If a liquid of such an azeotropic mixture is evaporated, we can get a vapor phase that has exactly the same molar concentration as the liquid. A solution of 96.5% ethanol with water is

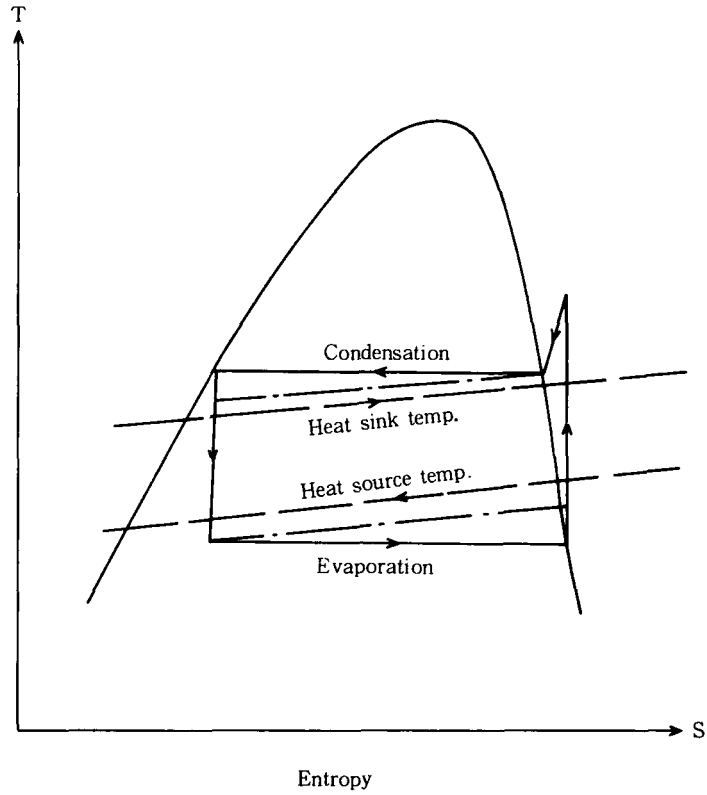

FIG. 28. Condensation and evaporation in thermodynamic cycle.

an example of an azeotropic mixture. A mixture that is not azeotropic is called nonazeotropic mixture. Condensation of a vapor of an azeotropic mixture can be treated as condensation of a pure vapor. Discussion of this is not within the scope of this section.

Figure 29 is a typical phase diagram of a nonazeotropic binary fluid composed of species A and B. The temperature is taken on the vertical axis and the concentration of component B is taken on the horizontal axis. Two curves are drawn in the figure. The upper curve is called the vapor-phase line and the lower one is called the liquid-phase line. These lines take different shapes depending on combinations of components and pressure. Temperatures $T_{S,A}$ and $T_{S,B}$ are the saturation temperatures of pure components A and B, respectively. When a binary mixture, of which the concentration of the B component is c_P, at temperature T_0 is cooled down to T_1, condensation initiates. However, the concentration of the condensed phase is different from

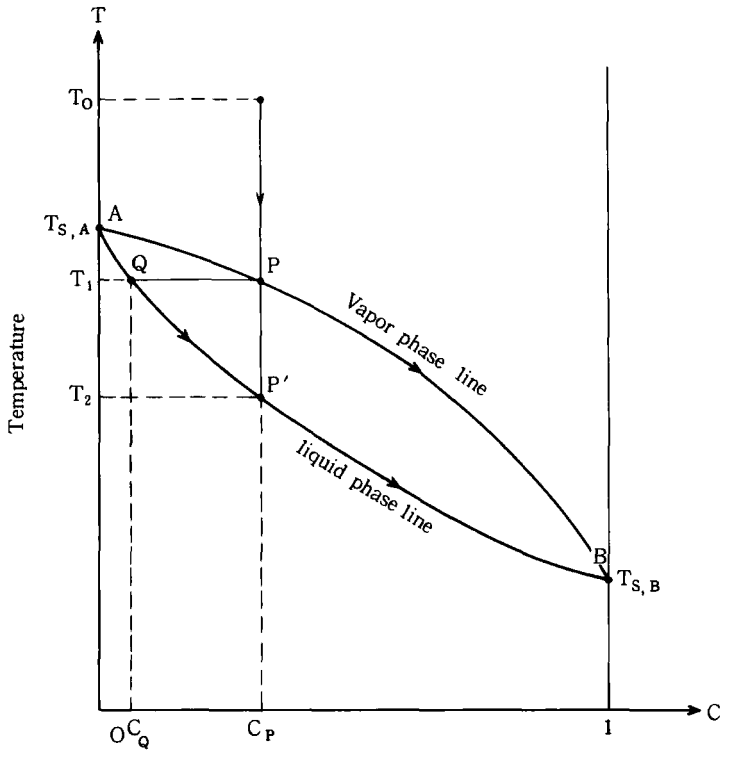

FIG. 29. Phase diagram of a binary mixture.

that of the vapor. The liquid phase formed at this stage corresponds to the point Q, of which the concentration of B component is c_Q, where $c_Q < c_P$, meaning that the liquid formed is richer in the A component. When a finite amount of vapor is condensed at a constant pressure, the concentration of the A component tends to decrease by condensation. Then, the vapor-to-liquid phase change occurs from the point P along the vapor-phase line down to the point B. The condensate changes its concentration along the line Q–P′–B, if cooling continues. This means that the condensation temperature of the binary mixture changes from T_1 to T_2 to $T_{S,B}$ along with the change of the concentration ratio of both components during the progress of condensation.

Such a phenomenon can be utilized to reduce the loss of available energy in a thermodynamic cycle by decreasing the average temperature difference for

heat exchange (Fig. 28). If an appropriate binary substance is chosen, and if the phase-change temperature is varied continuously during evaporation or condensation so as to keep constant the difference between the temperature of the heat source (or sink) and the evaporation or condensation temperature, the irreversibility caused by heat transfer can be reduced.

In Japan, a project named "Super Heat Pump and Energy Accumulation Systems," promoted by the Ministry of International Trades and Industries, started in 1984. In this project, success or failure of the development of a high-performance heat pump, aiming at a coefficient of performance as high as eight, is largely dependent upon the effective use of multicomponent working fluids.

A problem pertinent to the use of two-component fluids is in the heat transfer performance. The two-component media to be chosen for practical application are nonazeotropic mixtures, in most cases from a standpoint of improvement of the efficiency of the thermodynamic cycle, as stated previously. When a vapor of such a mixture is condensed, one of the components that has a lower dew point behaves like a noncondensable gas, and thus possibly brings about deterioration of heat transfer performance, as in the case of condensation of steam–air mixtures. Therefore, a couple of important issues concerning the research objectives of the condensation of a two-component vapor are raised: (1) prediction of characteristics of condensation heat transfer and (2) a technique for avoiding deterioration of (and, if possible, enhancing) condensation heat transfer.

As to the first item, an analytical procedure similar to the one employed for a vapor–noncondensable gas mixture can be used. However, obtaining a proper solution is more difficult, because the phase equilibria as shown in Fig. 29 should be taken into consideration for each combination of components. Fujii and Kato [98] have proposed formulas to calculate heat transfer and condensation rates for the case of condensation of a binary vapor on a vertical flat plate. Flows of both vapor and condensate are assumed to be laminar and the liquid phases of both components are considered to be miscible.

1. *Forced Convection Condensation*

If the total pressure P of the vapor mixture, the bulk mass concentration $W_{1\infty}$ of component 1, and the wall temperature T_w are given, the interface temperature T_i, the mass concentration W_{1i} of component 1 at the interface, the mass concentration W_{1L} of component 1 in the liquid phase, and the nondimensionalized rates of condensation of both components $\dot{M}_{11}$ and $\dot{M}_{21}$ are derived from Eqs. (61)–(63) using two equations expressing the

vapor-phase and the liquid-phase lines in the phase diagram. Then, the average heat flux $\dot{q}$ and the average mass flux of condensation $\dot{m}$ are obtained from Eqs. (64) and (65).

$$\frac{W_{1i}\dot{M}_{2l} - (1 - W_{1i})\dot{M}_{1l}}{W_{1i} - W_{1\infty}} R\,\mathrm{Sc} = 0.460\left(1 + \frac{W_{1\infty} - W_{1L}}{W_{1i} - W_{1L}}\right)^{-0.48} \times \left(\frac{W_{1\infty} - W_{1L}}{W_{1i} - W_{1L}}\right)^{-0.52} \mathrm{Sc}^{0.32} \tag{61}$$

$$\frac{\mu_L(\Delta h_1 \dot{M}_{1l} + \Delta h_2 \dot{M}_{2l})}{\lambda_L(T_i - T_w)} = 0.433\left[1.367 - \frac{0.432}{\sqrt{2R(\dot{M}_{1l} + \dot{M}_{2l})}} + \frac{1}{2R(\dot{M}_{1l} + \dot{M}_{2l})}\right]^{1/2} \tag{62}$$

$$\dot{M}_{2l}/\dot{M}_{1l} = (1 - W_{1L})/W_{1L} \tag{63}$$

$$\dot{q} = 2(\Delta h_1 \dot{M}_{1l} + \Delta h_2 \dot{M}_{2l})\frac{\mu_L}{l}\mathrm{Re}_{Ll}^{1/2} \tag{64}$$

$$\dot{m} = 2(\dot{M}_{1l} + \dot{M}_{2l})\frac{\mu_l}{l}\mathrm{Re}_{Ll}^{1/2} \tag{65}$$

where μ_L and λ_L are the viscosity and the thermal conductivity of the liquid mixture, respectively, Δh is the latent heat of condensation, R is the $\rho\mu$ ratio that appeared before, Sc is the Schmidt number, l is the length of the plate, Re_{Ll} is the two-phase Reynolds number ($=U_{\infty l}/\nu_L$), and $\dot{M}$ is the dimensionless mass flux ($=\dot{m}l/\mu_L(\sqrt{\mathrm{Re}_{Ll}})$.

2. *Natural Convection Condensation*

$$\frac{[W_{1i}\dot{M}_{2l} - (1 - W_{1i})\dot{M}_{2l}]R}{(W_{1i} - W_{1\infty})^{5/4}\Omega_w^{1/4}} = \sqrt{2}\,C(\mathrm{Sc})^{-3/4}\left(1 + \frac{W_{1\infty} - W_{1L}}{W_{1i} - W_{1L}}\right)^{-0.5} \times \left(\frac{W_{1\infty} - W_{1L}}{W_{1i} - W_{1L}}\right)^{-0.3} \tag{66}$$

$$\frac{\mu_L(\Delta h_1 \ddot{M}_{1l} + \Delta h_2 \ddot{M}_{2l})}{\lambda_L(T_i - T_w)} = 0.63(\ddot{M}_{1l} + \ddot{M}_{2l})^{-1/3} \tag{67}$$

$$\dot{q} = \frac{4}{3}(\Delta h_1 \ddot{M}_{1l} + \Delta h_2 \ddot{M}_{2l})\frac{\mu_L}{l}\mathrm{Ga}_l^{1/4} \tag{68}$$

$$\dot{m} = \frac{4}{3}(\ddot{M}_{1l} + \ddot{M}_{2l})\frac{\mu_L}{l}\mathrm{Ga}_l^{1/4} \tag{69}$$

$$\Omega_w = \frac{M_1 - M_2}{M_1 - (M_1 - M_2)W_{1\infty}} \tag{70}$$

$$C(\mathrm{Sc}) = \frac{3}{4}\left(\frac{\mathrm{Sc}}{2.4 + 4.9\sqrt{\mathrm{Sc}} + 5\,\mathrm{Sc}}\right)^{1/4} \tag{71}$$

where M is the molecular mass, Ga is the Galileo number, and $\ddot{M}$ is another dimensionless mass flux ($=\dot{m}l/\mu_L\,\mathrm{Ga}_l^{1/4}$).

Modification of the above equations for application to a horizontal tube has been given by Goto and Fujii [100]. Also, the above equations are applicable to the case when one of the two components is a noncondensable gas. In that case, we must put $\dot{M}_1$(or $\dot{M}_1$(or $\ddot{M}_1$) $= 0$ and $W_{1L} = 0$.

As mentioned, the heat transfer coefficient of condensation of a binary (or multicomponent) vapor is lower than that of pure vapor, because of the accumulation of the more volatile component on the liquid–vapor interface. The effect is more prominent in the case of natural convection condensation than in the case of forced convection condensation. Therefore, to raise the vapor velocity is an effective means to avoid deterioration of the condensation heat transfer of a binary vapor.

VI. Enhancement of Condensation Heat Transfer

A. Introduction

In principle there are only a couple of ways of enhancing condensation heat transfer, one is to increase the area of the condensing surface, and the other is to reduce the thermal resistance due to the condensate film formed on the surface. The former is realized by the use of extended surfaces, such as finned or fluted surfaces, and has been employed for a long time. However, because the heat transfer coefficent of condensation is in itself rather high, the use of high fins is not so efficient when the fin efficiency is considered. Low fins are used in most of the cases. As for reducing thermal resistance, some effort is required to reduce the thickness of the condensate film by various means, as will be shown in this section. In practice, a combination of these two methods, i.e., the use of flow fins and techniques of reducing the film thickness, is employed simultaneously to develop high-performance condenser surfaces.

B. Enhancement by Surface Tension Force

1. *Basic Principle*

Surface tension is rather a small force compared with other forces affecting heat transfer processes. It has not been positively taken into consideration

when condensation heat transfer is discussed. In reality, however, surface tension force is one of the most important items to be considered when enhancement of condensation heat transfer is at issue. Utilization of surface tension force is the most sophisticated way to enhance condensation, because no extra energy is needed to reduce the thickness of the condensate film.

Use of dropwise condensation, if possible, might be the most desirable among the surface tension-aided means of enhancement of condensation. If the condensing surface is not wetted by the condensate, the condensed liquid gathers together to form separate drops, leaving bare parts of the solid surface where the thickness of the liquid film is zero, and an extremely high heat-transfer rate is available, as discussed in Section III.

To our great regret, however, dropwise condensation has never been applied to industrial condensers. The reason is, as stated previously, that maintaining dropwise condensation for a long period of time has not yet been successful. It seems that to manufacture a permanent hydrophobic surface for the dropwise condensation of steam is not entirely impossible. However, to promote dropwise condensation of refrigerants, such as freons, seems difficult. In the following discussions, film condensation is considered as the mode of condensation occurring on the condensing surface.

Probably Gregorig[101] was the first person to propose that surface tension could be effective in enhancing heat transfer by condensation. Gregorig's work was on film condensation on a vertical fluted tube, of which the cross-section is illustrated in Fig. 30.

When a vapor condenses on such a surface, condensate forms a thin film over the profile of the solid wall. As is well known, when a liquid surface has a curvature, there arises a pressure difference between the fluids at both sides of the vapor–liquid interface. This pressure difference ΔP is described by the Laplace equation below:

$$\Delta P = \sigma(1/R_1 + 1/R_2) \tag{72}$$

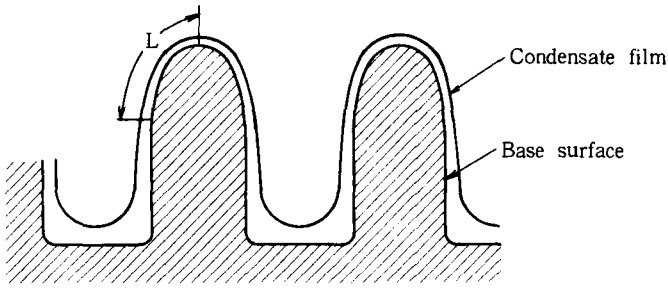

FIG. 30. Vertical, fluted surface studied by Gregorig.

where σ is the surface tension of the liquid and R_1 and R_2 are the principal radii of curvature at the point. A positive ΔP in Eq. (72) signifies that the pressure in the liquid is higher than the pressure outside.

In the case of Fig. 30, the pressure in the liquid film at the tip of the fin is higher than the ambient vapor pressure, because ΔP in Eq. (72) is positive since R_1 takes a finite positive value and R_2 is infinity. On the other hand, the pressure in the liquid film at the bottom of the groove between the fins is lower than the ambient pressure, because R_1 is negative there. Therefore, the liquid on the fin tends to move from the tip to the groove because of the pressure gradient along the film. As a result, the thickness of the condensate film at the fin tip is reduced and the liquid acccumulates in the bottom of the groove. The flow rate of the condensate toward the bottom depends upon the pressure difference and the distance between the tip and the bottom of the fin.

Gregorig described a shape of the fin for a convex profile, which provides a constant film thickness over the arc. The required shape of the vapor-liquid interface is

$$1/R = 0.75\pi/L[1 - (x/L)^2] \tag{73}$$

where R is the radius of curvature of the interface, x is the distance along the interface measured from the tip, and L is the arc length. Eq. (73) shows that R is smallest at $x = 0$ and grows to infinity at $x = L$. It should be noted that, although the flow of condensate considered here is restricted to the one occurring on the horizontal plane, the gravitational force drains the condensate vertically downward in the actual situation.

The ratio of gravity to surface tension force is represented by a nondimensional parameter called the Bond number. If R is taken as the characteristic length, the Bond number is

$$\mathrm{Bo} = R^2(\rho_l - \rho_v)g/\sigma \tag{74}$$

If the physical properties of water are assumed, $\mathrm{Bo} \sim 10^{-3}$ when $R = 0.1$ mm, and $\mathrm{Bo} \sim 0.1$ when $R = 1$ mm. This means that the flow of condensate at the tip of a fin is governed mainly by surface tension force, as long as the radius of curvature there is less than 1 mm.

2. *Optimum Fin Geometry for Vertical Condenser Tube*

More elaborate work on the enhanced condensation on fins was carried out by Hirasawa *et al.* [102–105]. They solved the equations of momentum and energy for the condensate film both at the fin tip, with a small radius of curvature, and in the groove, for fins with three different geometries, as shown in Fig. 31. Using the results they obtained, they determined the optimum fin

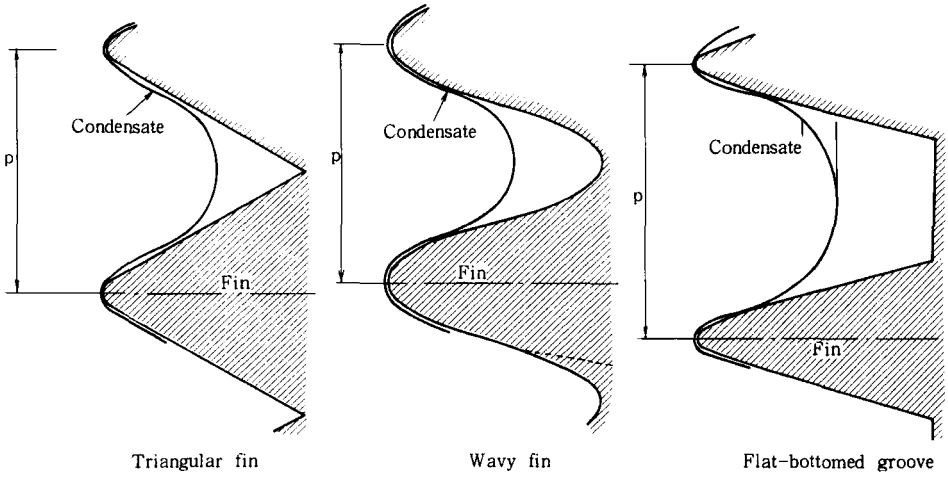

FIG. 31. Geometries of fins.

profile and the optimum interval of the drainage disk fitted to a vertical condenser tube as shown in Fig. 32. The role of the drainage disk here is to remove the condensate, which fills up the grooves and reduces the effective area for condensation.

Shown in Fig. 33 is one of their results. The heat transfer coefficient averaged over the interval of the drainage disk is plotted against the fin pitch for three different geometries. It is assumed that R113 is condensed under a vapor-to-surface temperature difference of 10 K. Height of the fin is 0.61 mm for all the geometries. It is seen that the maximum value of the heat transfer coefficient exists for every geometry at a fin pitch of 0.5–0.6 mm. At a lower fin pitch, the grooves are filled with condensate, while at a larger fin pitch, the relative area of the bottom of groove, which is ineffective for condensation, becomes larger than the area of the fin tip. Such a tendency is more remarkable for the fin with a flat bottom. The maximum heat transfer coefficient is more than 10 times that of a smooth tube calculated by the Nusselt theory. It is estimated that the factor of about 2.5 out of 10 is owing to the increase of surface area and the rest is due to the contribution of the surface tension and drainage disk.

A variety of high-performance condenser tubes, which have minute fins with sharp tips, have been developed and used in refrigerators and air-conditioning devices. The mechanism of condensation enhancement in those tubes is basically the same as discussed here, though alignments, geometries, and dimensions of fins are somewhat different among different manufacturers.

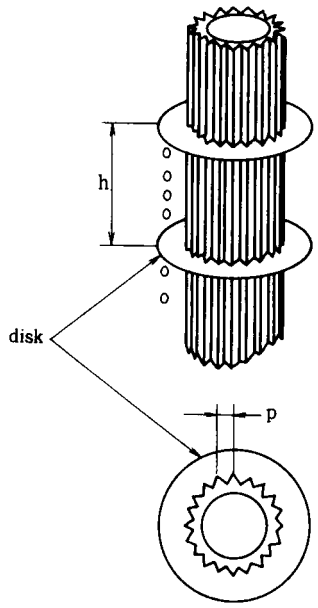

FIG. 32. High-performance longitudinal fin tube with drainage disks.

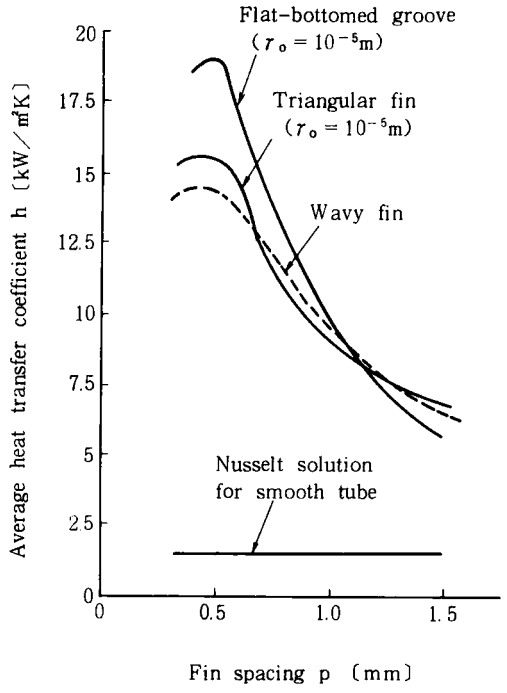

FIG. 33. Experimental results using a longitudinal fin tube. R-113, $T_s - T_w = 10$ K, $l_b = .61$ mm, $h = 50$ mm.

3. *Horizontal Low-Fin Tube*

Use of horizontal tubes instead of vertical tubes seems much more frequent in condensation of vapor in industrial devices. Also, in this case, low-fin tubes (integral-fin tubes) are employed to enhance condensation. As mentioned, extension of surface area by fins and reduction of the thickness of condensate film by surface tension are simultaneous goals. However, these two effects sometimes are not compatible. That is to say, if one reduces too much the pitch between fins to increase the surface area, the condensate is flooded in the grooves, resulting in reduction of the effective surface area. It is known that the tendency for the condensate to collect in the interfin space depends on the surface tension σ and the density ρ_l. The larger the ratio σ/ρ_l, the more likely the condensate accumulates. The degree of condensation heat transfer enhancement compared with the smooth surface decreases for substances having larger σ/ρ_l values.

If we measure the position up to which the space between the fins is flooded with the condensate by the azimuthal angle from the bottom centerline of the tube, and call it the retention angle (denoted Φ), this Φ must be determined from the surface tension and the density of condensate and the dimensions and geometries of the tube and fins. Several authors, e.g., Honda and colleagues [106,107] and Ruby and Webb [108], derived, under some assumptions, an expression for Φ. For example, in the case of rectangular shaped fins, their expression yields

$$\Phi = \cos^{-1}[1 - 4(\sigma/\rho_l)/(Dgp)] \tag{75}$$

where D is the tube diameter and p is the spacing between the fins. It is seen, by examining Eq. (75), that the values of σ/ρ_l and the fin spacing p are very important values for flooding. Equation (75) is plotted in Fig. 34 for a tube with a diameter D of 14.7 mm and for three values of σ/ρ_l. Clearly, a high-surface-tension liquid such as water floods very well a finned tube at relatively small fin spacings, whereas for a low-surface-tension liquid such as freon, the fin spacing can be decreased considerably before complete flooding occurs.

Masuda and Rose [109] measured the dependency of the enhancement ratio on fin spacing and condensate flooding. Shown in Fig. 35 is their result. The enhancement ratio on the ordinate is the one taken under the condition that the vapor-to-wall temperature difference ΔT is the same. Thirteen integral-fin tubes with a root diameter of 12.7 mm were used. Fins were rectangular shaped, having the same fin thickness (0.5 mm) and height (1.6 mm). Tests were carried out at near-atmospheric pressure and downward vapor flow with velocities between 0.5 and 1.1 m/sec. The fin spacing at which the maximum enhancement ratio was obtained differs depending on fluid. It is 1.5 mm for steam, 1.0 mm for ethylene glycol, and 0.5 mm for R113. The

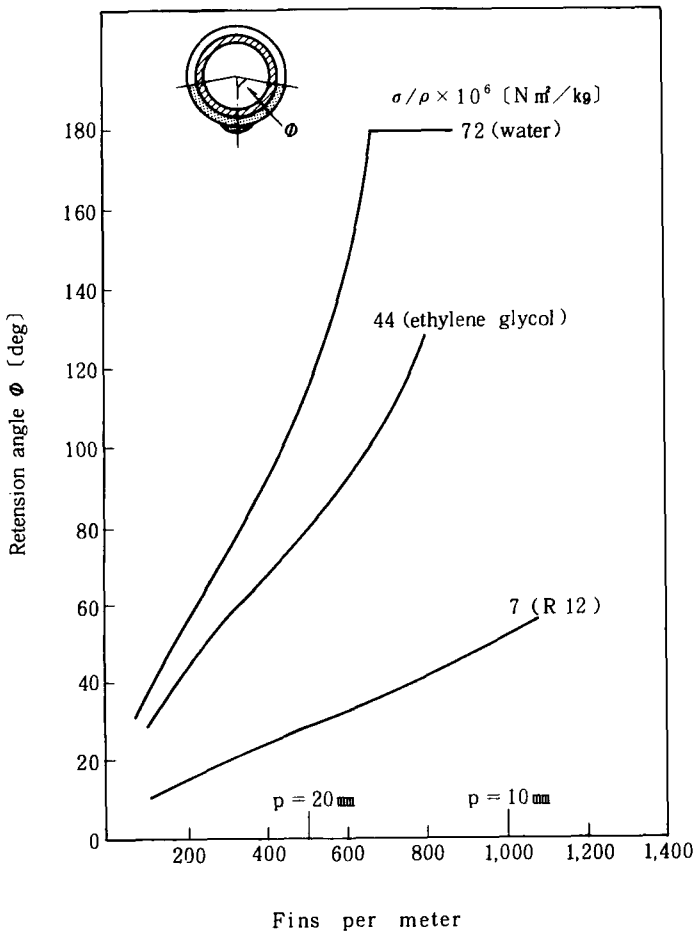

FIG. 34. Dependence of retention angle on fin spacing.

values of the maximum enhancement ratio decrease in the order of R113, ethylene glycol, and steam. The percentage numbers for each data point correspond to the percent flooding calculated using Eq. (75). As expected, the maximum enhancement ratio increases and the optimum fin spacing decreases with the decrease of σ/ρ_l value.

A rather complicated mathematical treatment would be required to make a theoretical prediction of the performance of a horizontal integral-fin tube. Equations of flow and heat transfer should be solved simultaneously under complexed geometrical, thermal, and fluid dynamical conditions. However, a prediction method proposed by Honda and Nozu [110] and Honda *et al.*

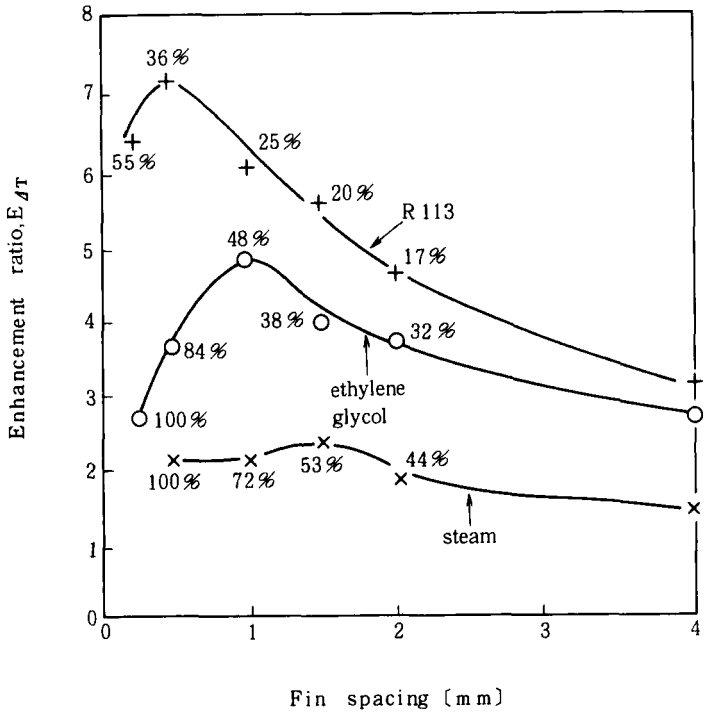

FIG. 35. Dependence of enhancement on fin spacing and condensate flooding.

[111] gives a little less complicated procedure for obtaining the performance of a low-fin tube. They distinguished a finned tube by two regions: one is the region where the interfin space is not flooded with the condensate and the other is the region flooded with the condensate [Fig. 36]. The two regions can be divided by the retention angle mentioned before. Then, they made models simulating the flow of condensate in the interfin spaces and they calculated the heat transfer rates. Comparison of their results of calculation with experimental data (e.g., Masuda and Rose [109]) showed fairly good agreement, and the effect of the fin spacing could be predicted correctly for fluids having different σ/ρ_l values.

Honda *et al.* [106] and Honda and Nozu [107] have proposed a technique for enhancing condensation of vapors, the liquid phases of which have large values of σ/ρ_l. Their idea was to attach a porous drainage plate to the bottom of the horizontal finned tube, reducing the condensate retention between the fins and increasing the effective area for condensation, thus enhancing the condensation heat transfer by the actions of surface tension and gravitational forces.

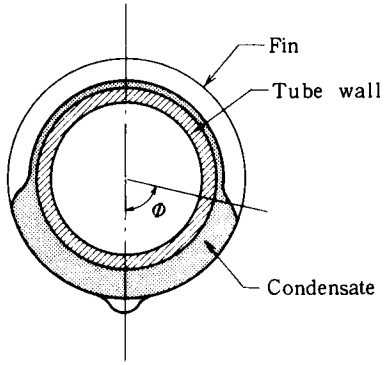

FIG. 36. Physical model of condensation on a low integral-fin tube.

In the experiment the authors prepared finned tubes of 19 mm outer diameter and four different fin profiles. Their heights were 0.92–1.46 mm and the pitches were 0.50–0.98 mm. The drainage plates were 1.9 mm thick and 14–19 mm wide and were made of porous nickel of 0.8 mm pore diameter and 490 kg/m^3 bulk density. One of those plates was inserted in a 2-mm-wide and 1- to 1.5-mm-deep groove machined along the bottom of the finned tube.

Figure 37 illustrates how effective such a drainage plate is. The fluids used are (a) methanol and (b) the refrigerant R113. For both fluids, aspects of condensation on finned tubes without porous drainage plates are shown. The degree of surface subcooling is kept constant at about 8 K. Horizontal arrows on the left-hand sides of the pictures indicate the positions at which the thickness of the condensate film changes greatly and the curvature of the film turns from convex to concave. It means that the grooves between the fins beneath this position are flooded with condensate. The pictures suggest that this position moves toward the bottom of the tube by attaching the drainage plate. Comparison between methanol and R113 reveals that flooding occurs at a higher position for methanol than for R113, and the effect of the drainage plate is also larger for methanol, which has a greater σ/ρ_l value. These results clearly indicate the effectiveness of drainage plates. The issues to be discussed before they are used in industrial condensers may be the cost of manufacturing.

4. *Other Methods of Enhancement*

Although details will not be mentioned, there are some other methods of enhancement of condensation heat transfer utilizing surface tension force.

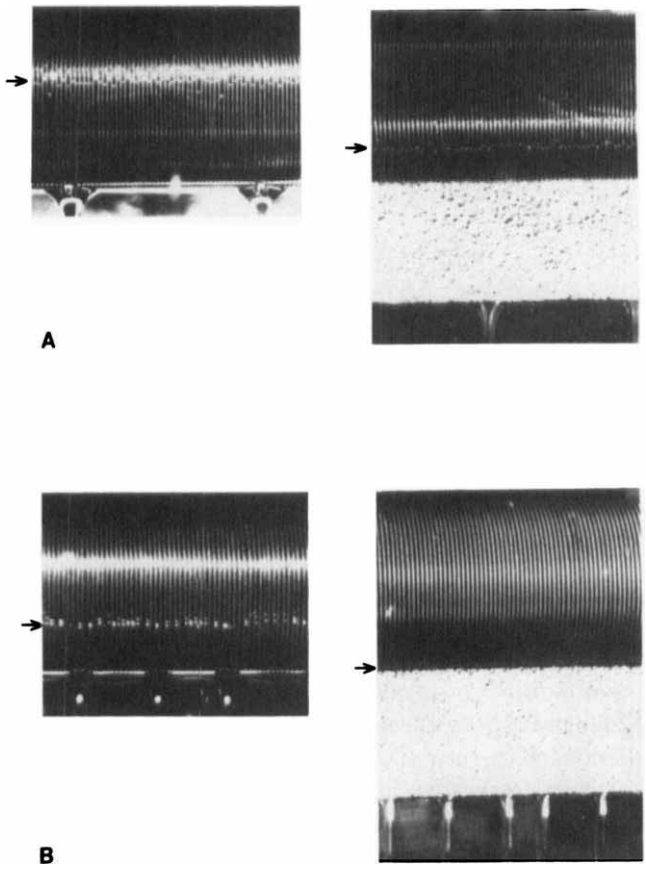

FIG. 37. Effect of porous drainage plates for enhancement of condensation on a low-fin tube. (A), Methanol; (*left*), without porous drainage plate; (*right*), with 14 mm high drainage plate. (B), R113; (*left*), without porous drainage plate; (*right*), with 15 mm high drainage plate. [Courtesy of Prof. Hiroshi Honda, Kyushu University.]

One of them is to wind a wire around the tube. This method seems to have been proposed first by Thomas [112] in 1967. The wires, with a circular or rectangular cross-section, when wrapped around the tube, attract and retain the condensate, thus reducing the thickness of the liquid film on the surface in between them. There must be an optimum value of the pitch of winding, because too large or too small a pitch would reduce the effect. Fujii *et al.* [113] carried out an experiment and analysis for the case of natural convection condensation and found that the maximum rate of enhancement was attained when the ratio of the wire diameter to the pitch was about 1:2. The enhancement ratio obtained was about three when compared with condensation

on the bare tube, though the value was dependent upon the liquid and the diameter ratio.

As another effort to reduce the average condensate thickness, use of non wettable strips has been proposed. For example, Glicksman *et al.* [114] conducted measurements on condensation of steam on a single horizontal tube on which various strips of PTFE were placed. According to their result, enhancements as large as 100% were observed at low heat fluxes when the strip was placed longitudinally along the bottom of the tube.

Kumagai and colleagues [115,116] manufactured special condensing surfaces on which hydrophobic and hydrophilic parts exist alternately. They measured the heat transfer characteristics on these surfaces, where dropwise and film condensation occurred simultaneously. As a matter of course, the local heat transfer coefficient is higher on the parts where dropwise condensation occurs and lower where film condensation takes place. However, they found that, under a certain condition, the heat transfer coefficient of the film condensation area was increased, due possibly to a disturbance caused by drops absorbed into the condensate film from the dropwise condensation area. These authors have suggested that this mechanism could be employed for high-performance condenser surfaces.

There still remain a variety of proposed techniques for enhancement of condensation heat transfer. Also, there are a number of review papers regarding this subject. Interested readers are advised to refer to some of them [88,117–120].

C. ENHANCEMENT BY ELECTRIC FIELD

1. *Basic Principle*

According to Bergles [117], the techniques of heat transfer enhancement in general can be classified into three categories: (1) passive technique, (2) active technique, and (3) combined technique. The passive technique needs no extra energy to enhance heat transfer. Use of extended surfaces is one of the typical examples of this technique. The active technique requires an extra power supply for heat transfer enhancement. As proposed, though not always successfully, by some people, use of a wiper or scraper to remove the condensate film is an example of the active technique. Also, utilization of an electric field, to be described in the following discussion, is another example. The combined technique is, literally, the combination of the two methods. If a finned surface is used under an electric field, both the passive and and active techniques are employed simultaneously.

Generally speaking, as Bergles has insisted, the active technique is less preferable in many cases, because the consumption of extra power for heat

transfer enhancement is likely to mar the gain. However, in case the amount of power consumed is much less than the advantage expected by the active enhancement, it is worthwhile to consider. Enhancement of condensation by an electric field is very effective when the condensed liquid has a low electrical conductivity.

When a fluid with dielectric constant ε is placed under an electric field $\mathbf{E}$ (which is a vector quantity), the body force $\mathbf{f}$ acting on the fluid is expressed as below [121]:

$$\mathbf{f} = \rho_e \mathbf{E} - \frac{1}{2} E^2 \nabla \varepsilon + \frac{1}{2} \nabla \left(E^2 \rho \frac{\partial \varepsilon}{\partial \rho} \right) \tag{76}$$

The first term on the right-hand side of this equation represents the Coulomb force acting on the free electric charge ρ_e, the second term is the force due to the spatial variation of dielectric constant ε, and the third term is generated from the spatial change of the electric field intensity. In most liquids, the sum of the second and the third terms, representing the force acting on the electric charges by polarization, is important because ρ_e is almost negligible.

The basic principle of the heat transfer enhancement by electric field is to utilize the body force mentioned above to modify the flow and the temperature distribution in the vicinity of the heat transfer surface. How to use the electric field may change depending upon the mode of heat transfer, fluid, geometry, purpose of heat transfer enhancement, and other conditions. Theoretical treatment of this techique is rather complex, because the interaction between electrical, thermal, and flow fields must be considered. Sometimes this technique is called electrohydrodynamic (EHD) enhancement. A detailed description of the EHD technique applied to the other modes of heat transfer is given by Jones [122].

If we focus attention on the EHD enhancement of condensation heat transfer, the applied electric field can be effective in two ways. One is that the electric field induces convective motion in the layer of condensate liquid, and the other is that the vapor–liquid interface is rendered unstable by the electric force. However, the former does not seem to be very effective. Perhaps it is because of the difficulty in inducing strong convection, sufficient to increase appreciably the heat transfer rate, in so thin a liquid film. The latter principle seems more promising.

2. *Enhancement of Condensation by EHD Instability of Vapor–Liquid Interfaces*

When an external electric field is applied to a body of fluid, the distribution of electric charges is altered. The transient process for redistribution of electric charges is described by an equation as below, which is derived from the

Maxwell equations for electromagnetic fields:

$$D\rho_e/Dt + (\sigma_e/\varepsilon)\rho_e = 0 \tag{77}$$

where σ_e is the electrical conductivity of the fluid. Here, both σ_e and ε are assumed to be constant.

Equation (77) tells us that the electric charge density ρ_e decreases with time in proportion to $\exp[-(\sigma_e/\varepsilon)t]$. That is to say, the characteristic time of the electric charge distribution due to a change of the electric field distribution is

$$\tau = \varepsilon/\sigma_e \tag{78}$$

This time constant τ is called the relaxation time and is a measure of the electric field tendency to be steady. Approximate values of τ for liquids are as follows: water, ~ 1 μsec; ethanol, ~ 10 μsec; R113, ~ 10 sec.

When an electric field is imposed on a liquid for periods much longer than the relaxation times, the electric charges in the liquid are distributed so that the electric field inside may become substantially zero except at the liquid surface. In case one of the electrodes is placed in the liquid and the other is in the gaseous phase, as shown in Fig. 38, the electric potential in the liquid is everywhere homogeneous, being nearly equal to the potential on the electrode immersed in the liquid. If an electric potential is applied between these two electrodes, a stress called Maxwell stress acts on the gas–liquid interface. The Maxwell stress in the case of Fig. 38 is normal to the interface and is equal to $(1/2)\varepsilon_g E^2$, *where* ε_g is the dielectric constant of the gas phase.

Let us consider here the stability of the gas–liquid interface. The forces acting on the interface are gravitational, capillary, and electrical forces, if the liquid is quiescent. The first two forces tend to stabilize, and the last one to

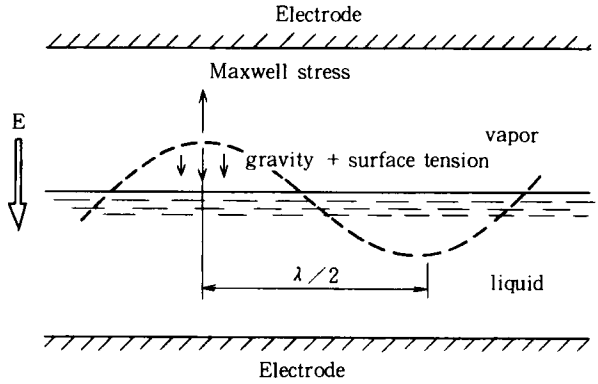

FIG. 38. Stability of a liquid surface under an electric field.

destabilize, the interface. If, by some disturbance, the liquid surface deforms as shown in Fig. 38, the Maxwell stress at the peak of the surface increases, because the distance from the upper electrode is reduced. At the same time, the gravitational potential and the capillary force on the curved interface act to pull down the surface. The interface becomes unstable when the attractive force by the upper electrode exceeds the pull-down forces. The criterion for onset of instability can be obtained by solving a modified Rayleigh–Taylor instability problem, which includes the contribution of electric field.

The equation to be solved to derive the instability criterion is as below. Detailed explanation is omitted here but is given elsewhere (e.g., see Ref. [123]).

$$\sigma m^2 - 8.85 \times 10^{-12}\varepsilon_v(E/\delta)^2 m \coth(m\delta) + (\rho_l - \rho_v)g = 0, \qquad m = 2\pi/\lambda \quad (79)$$

where ε_v is the dielectric constant of the vapor phase and δ is the distance between the liquid surface and the electrode above the liquid. The wavenumber m obtained from Eq. (79) represents the unstable wavenumber at which the liquid–vapor interface becomes unstable. It should be noted that in Eq. (79) an assumption is made that the gravitational force is in the direction of vertically downward, whereas the liquid surface faces horizontally upward.

Equation (79) has two asymptotic solutions for two extremes, $m \to \infty$ and $m \sim 0$. For $m \sim 0 (\lambda \to \infty)$

$$E^2 = \frac{(\rho_l - \rho_v)g\delta^3}{8.85 \times 10^{-12}\varepsilon_v} \quad (80)$$

and for $m \to \infty (\lambda \sim 0)$

$$\lambda = \frac{2\pi\sigma}{8.85 \times 10^{-2}\varepsilon_v(E/\delta)^2} \quad (81)$$

The value of E expressed by Eq. (79) represents the electric field potential above which the liquid surface with inifinite expanse becomes unstable. The surface with a finite expanse needs a stronger electric field to be destabilized. Solutions for other values of m, between 0 and infinity, are obtained numerically.

Figure 39 shows the dependence of the unstable wavelength λ on the applied electric voltage. In general, the unstable wavelength tends to decrease with the voltage. It means that the liquid surface becomes unstable more easily under a stronger electric field. However, if we observe Fig. 39 more closely, we find that there appear minimum values of electric voltage where the distance δ is large (in Fig. 39, $\delta > 3$ mm). These minimum values make determination of the unstable wavelengths a little complex. For example, if the dimension of the liquid surface is 20 mm, the intersections of the horizontal line at 2×10^{-2} m (drawn in Fig. 39) with the curves obtained by calculation

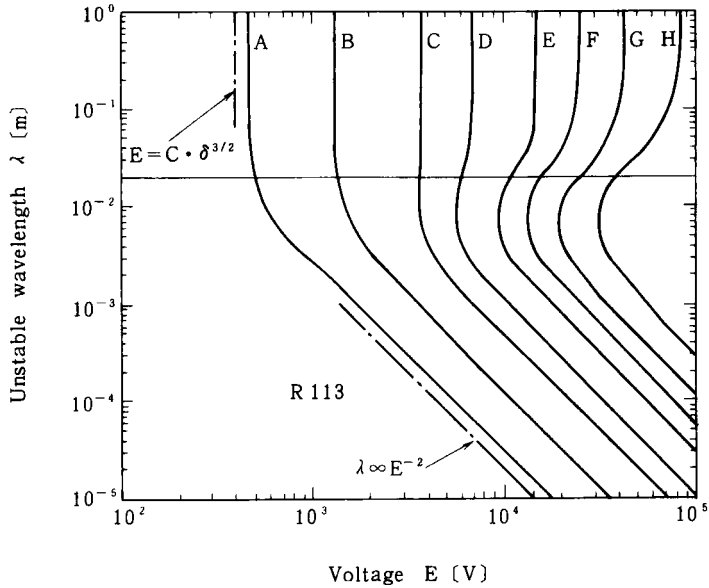

FIG. 39. Dependence of unstable wavelength on an applied electric field. Distance δ: A, 0.5 mm; B, 1 mm; C, 2 mm; D, 3 mm; E, 5 mm; F, 7 mm; G, 10 mm; H, 16 mm.

give the critical electric voltage over which the liquid surface becomes unstable, as long as the curves have no minimum values of E. Then, the critical values of E are above 500 V for $\delta = 0.5$ mm, 1040 V for $\delta = 1$ mm, and 2800 V for $\delta = 2$ mm. However, for $\delta = 3$ mm, the critical value of E is not 6500 V (corresponding to the intersection) but 5500 V corresponding to the minimum value of E. At any rate, the liquid surface can be unstable under an electric field with sufficient intensity. When the electric field intensity exceeds a certain critical value, a disturbance wave appears on the surface and it grows if the electric field is intensified. The principle described here is applicable to enhancing heat transfer by film condensation, unless the condensate liquid has a high electrical conductivity.

Choi [124] attempted to enhance film condensation by destabilizing the condensate film with a strong electric field. He observed that waves were generated by application of an electric field and enhancement of condensation heat transfer as high as three times the normal value was obtained.

Yabe *et al.* [125] confirmed that the liquid film of condensate was pulled toward an electrode when a nonuniform electric field was applied between the cylindrical surface of a vertical condenser tube and the electrode facing it because of an instability of the liquid layer. They used this phenomenon to

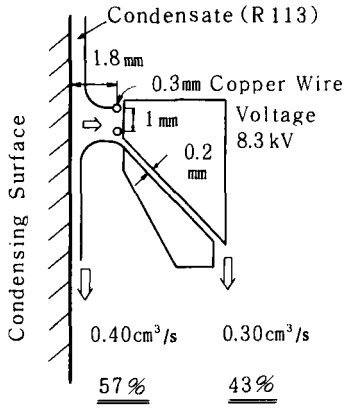

FIG. 40. Enhancement of condensation heat transfer by an electric field.

remove a portion of the condensate from the surface. Shown in Fig. 40 is the concept of such an idea. In this case wire electrodes are placed at a distance 1.8 mm from the condenser tube. An electrical potential of 8.3 kV was applied between the tube and the wire. As expected, the condensate was drawn toward the wire electrodes and was removed through a conduit placed behind the electrodes. This reduced the thickness of the condensate film, resulting in enhancement of condensation heat transfer. If electrodes and conduits for drainage were placed at a certain interval along the condenser surface, a considerable enhancement could be achieved.

What makes this method more efficient is that the electrical power consumed with this process can be very small (less than 1% of the amount of heat transmitted), because in the case of liquids with low electrical conductivity, such as freons, the current induced remains very small even if a high voltage is applied. On the basis of their fundamental study, Taketani *et al.* [126] developed this technique further for industrial applications with the use of thin, helical electrodes (Fig. 41). Furthermore, Yabe *et al.* [127] attempted to reduce still more the thickness of the condensate film on the areas of the condensing surface that did not stand opposite the helical electrodes. The means that the authors employed was a planer electrode, with which many protuberances of the condensate were formed on the liquid film when an appropriate electric field was imposed. The authors called this phenomenon pseudodropwise condensation, because the appearance resembled dropwise condensation. In the case of condensation of freon R114 on a vertical tube, an enhancement ratio of about 6 has been observed with the simultaneous use of the helical electrodes for pulling out the condensate and the planer electrodes for generating pseudodropwise condensation.

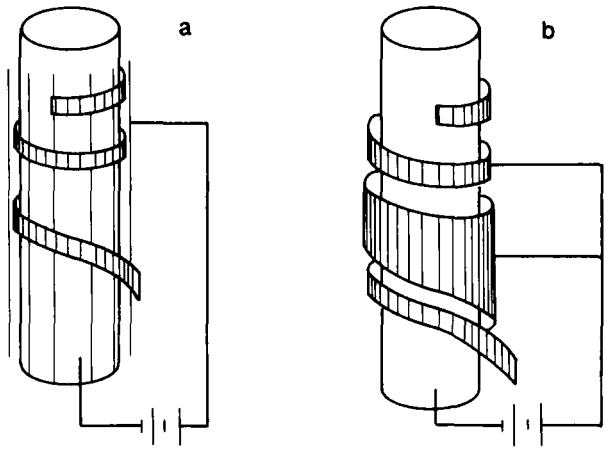

FIG. 41. Helical electrodes. (a), Helical wire with lattice electrode; (b), helical wire with plate electrode.

It should be noted that the results mentioned above were obtained under a nonuniform electric field. However, the present author believes that the electric field does not need to be nonuniform. As shown in Fig. 39, a uniform electric field with same intensity can have almost the same effect.

VII. Concluding Remarks

In closing this review the author would like to mention briefly some personal comments on the future trends in the progress of the condensation research. The order does not coincide with the order of sections.

1. *Film condensation of single-component vapors*: Numerical computation will be performed extensively assuming complicated boundary and thermofluid-dynamic conditions. More accurate and detailed results will be published on a variety of combinations of fluids and geometries. However, these will not contribute much to deepen our knowledge and understanding of the essential characteristics of the phenomenon.

2. *Film condensation of multicomponent vapors*: As stated previously, the need for research on film condensation of multicomponent vapors will increase in connection with the technological development of thermal energy conversion devices such as heat pumps. Numerical computation will be an efficient tool for investigation, though importance of experimental work will not decrease. Analytical approaches will be rather limited in this area. Obtaining experimental formulas, which are valid for a wide range of parameters,

will not be easy either, because there are too many variables to be taken into account. One of the important issues of this field is to obtain by some means the reliable and accurate values of relevant thermophysical properties of multicomponment fluids. From a practical point of view, to develop a technique for preventing deterioration and, if possible, enhancing condensation will be most urgently in demand.

3. *Enhancement of condensation heat transfer*: This will remain a subject that will interest many researchers. However, no great progress will be expected as long as the so-called passive techniques are concerned, because almost every mechanism of enhancement that we can imagine has already been developed. Thus, what seems to be left for us will be to pursue active (or combined) techniques such as the use of electric fields.

4. *Dropwise condensation*: As mentioned previously, the most important objective of dropwise condensation research is to manufacture surfaces on which dropwise condensation can be maintained for a sufficiently long period of time, even under industrial conditions. The other issues concerning heat transfer mechanisms are of minor significance, because a great deal of work on these issues has been performed during the past 25 years.

5. *Direct contact condensation*: This is an area not mentioned in this review. An insufficient number of studies has been carried out in this field. There remain a variety of interesting phenomena to study, such as are observed in direct contact condensation of immiscible components. However, the importance of any such investigation is largely dependent upon its practical application.

6. *Microscopic aspects of condensation research*: Understanding the condensation phenomenon from a microscopic view point will become more important in the future. The author's personal opinion is that one of the possible ways that condensation research can expand its territory is to pay attention to phenomena of molecular scale. By broadening our field of vision, we shall be able to get a deeper insight into the conventional process of condensation.

NOMENCLATURE

A	area, area ratio	Ga	Galileo number
Bo	Bond number	g	gravitational acceleration
C	specific heat	H_m	phase change number
c	molar concentration, specific heat	h	heat transfer coefficient, enthalpy
D	drop diameter, tube diameter, distance between nucleation sites	h_{fg}	latent heat of condensation
		Kn	Knudsen number
E	electric voltage, electric field intensity	k_l	liquid thermal conductivity
F	force	L	length, latent heat of condensation
Fr	Froud number	l	characteristic length
f	distribution function	M	molecular mass

$\dot{M}$	dimensionless mass flux
$\ddot{M}$	dimensionless mass flux
m	wavenumber
$\dot{m}$	mass flux
$N(r)$	drop size distribution function
Nu	Nusselt number
n	number density, index
P	pressure
Pr	Prandtl number
p	fin spacing
$\dot{q}$	heat flux
$\dot{q}_B$	heat flux through the base of a drop
R	gas constant, thermal resistance, $\rho\mu$ ratio, radius of curvature
Re	Reynolds number
R_{max}	maximum drop radius
R_{min}	minimum drop radius
r	radius
Sc	Schmidt number
T	temperature
t	time
U	velocity
V	velocity
v	specific volume
W	velocity, mass concentration
x	coordinate
z	coordinate

Greek Symbols

Γ	variable defined by Eq. (11)
δ	distance
ε	dielectric constant
θ	contact angle
κ	specific heat ratio
λ	unstable wavelength
μ	viscosity
ν	kinematic viscosity
ξ	variable defined by Eq. (27)
ρ	density
ρ_e	electric charge density
σ	surface tension, condensation coefficient
σ_e	electrical conductivity
τ	relaxation time
Φ	retention angle

Subscripts

a	adhesive
c	condensation, constriction, cohesive
e	evaporation, electrical
f	liquid film
g	gas
i	interface
L	liquid
l, l	liquid, characteristic length
m	mean
s	saturated, solid, surface
v	vapor
w	wall
∞	bulk, infinity

REFERENCES

1. R. Donaldson, ed., "Bicentenary of the James Watt Patent." Univ. of Glasgow, Glasgow, 1969.
2. W. Nusselt, Die Oberflächenkondensation des Wasserdampfes. *Z. VDI* **60,** 541, 569 (1916).
3. E. Schmidt, W. Schurig, and W. Sellschop, Versuche über die Kondensation von Wasserdampf in Film- und Tropfenform. *Tech. Mech. Thermodyn.* **1,** 53 (1930).
4. G. S. Springer, Homogeneous nucleation. *Adv. Heat Transfer* **14,** 281 (1978).
5. H. Merte, Jr., Condensation heat transfer. *Adv. Heat Transfer* **9,** 181 (1973).
6. S. Sideman and D. Moalem Maron, Direct contact condensation. *Adv. Heat Transfer* **15,** 228 (1982).
7. W. M. Rohsenow, Heat transfer and temperature distribution in laminar film condensation. *Trans. ASME* **78,** 1645 (1956).

8. W. M. Rohsenow, J. H. Webber, and A. T. Ling, Effect of velocity on laminar and turbulent-film condensation. *Trans. ASME* **78,** 1637 (1956).
9. E. M. Sparrow and J. L. Gregg, A boundary layer treatment of laminar-film condensation. *J. Heat Transfer* **81,** 13 (1959).
10. M. M. Chen, An analytical study of laminar film condensation: Part 1—Flat plate. *J. Heat Transfer* **83,** 48 (1961).
11. R. W. Schrage, "A Theoretical Study of Interface Mass Transfer." Columbia Univ. Press, New York, 1953.
12. W. M. Rohsenow, Film condensation of liquid metals. *Prog. Heat Mass Transfer* **7,** 469 (1973).
13. Y. S. Huang, Heat transfer by condensation of low pressure metal vapors. Ph.D. Thesis, Case Western Reserve Univ., Cleveland, Ohio, 1971.
14. G. S. Springer and A. J. Patton, A kinetic theory description of liquid–vapor phase change. *Int. Symp. Rarefied Gas Dyn., 6th* p. 1497 (1969).
15. D. A. Labuntzov, An analysis of evaporation and condensation process. *High Temp. (Engl. Transl.)* **5,** 579 (1967).
16. D. A. Labuntzov and A. P. Kryukov, Analysis of intensive evaporation and condensation. *Int. J. Heat Mass Transfer* **22,** 989 (1979).
17. A. T. Mills and R. A. Seban, The condensation coefficient of water. *Int. J. Heat Mass Transfer* **10,** 1815 (1967).
18. U. Narusawa and G. S. Springer, Condensation coefficient of water. *AEC Rep., USAEC* **COO-2032-6** (1972).
19. S. Hatamiya and H. Tanaka, A study on the mechanism of dropwise condensation (2nd Report: Condensation coefficient of water at low pressures) (in Japanese). *Trans. JSME, Ser. B* **52,** 2214 (1986).
20. S. J. Wilcox and W. M. Rohsenow, Film condensation of potassium using copper condensing block for precise wall temperature measurement. *J. Heat Transfer* **92,** 359 (1970).
21. R. Ishiguro and K. Sugiyama, An experimental study on potassium condensation (in Japanese). *Trans. JSME, Ser. B* **54,** 967 (1988).
22. S. Necmi and J. W. Rose, Heat-transfer measurements during dropwise condensation of mercury. *Int. J. Heat Mass Transfer* **20,** 877 (1977).
23. J. Niknejad and J. W. Rose, Interface matter transfer: an experimental study of condensation of mercury. *Proc. R. Soc. London, Ser. A* **378,** 305 (1981).
24. S. Fujikawa and M. Maerefat, A study of the molecular mechanism of vapor condensation (in Japanese). *Trans. JSME, Ser. B* **56,** 1376 (1990).
25. S. A. Stylianou and J. W. Rose, Dropwise condensation of ethanediol. *Int. J. Phys.-Chem. Hydrodyn.* **3,** 199 (1982).
26. J. W. Rose, On interphase matter transfer, the condensation coefficient and dropwise condensation. *Proc. R. Soc. London, Ser. A* **411,** 305 (1987).
27. E. J. Le Fevre, Personal communication to J. W. Rose (1966); see also Appendix 6 in J. W. Rose, Ph.D. Thesis, University of London, London, 1964.
28. I. Tanasawa, Dropwise condensation—The way to practical applications. *Proc. Int. Heat Transfer Conf., 6th* **6,** 393 (1978); see also Dropwise condensation—Progress toward practical applications. *In* "Heat Transfer Science and Technology" (B. X. Wang, ed.), p. 43. Hemisphere, New York, 1987.
29. M. Jakob, Heat transfer in evaporation and condensation—II. *Mech. Eng.* **58,** 729 (1936).
30. J. F. Welch and J. W. Westwater, Microscopic study of dropwise condensation. *Int. Dev. Heat Transfer, Proc. 1961–1962 Int. Heat Transfer Conf.* p. 302 (1963).
31. A. Umur and P. Griffith, Mechanism of dropwise condensation. *J. Heat Transfer* **87,** 275 (1965).

32. J. L. McCormick and J. W. Westwater, Nucleation sites for dropwise condensation. *Chem. Eng. Sci.* **20,** 1021 (1965).
33. D. W. Tanner, C. J. Potter, D. Pope, and D. West, Heat transfer in dropwise condensation—Part I. The effects of heat flux, steam velocity and non-condensable gas concentration. *Int. J. Heat Mass Transfer* **8,** 419 (1965).
34. C. Graham, The limiting heat transfer mechanism of dropwise condensation. Ph.D. Thesis, Massachusetts Institute of Technology, Cambridge, 1969.
35. E. J. Le Fevre and J. W. Rose, Heat-transfer measurement during dropwise condensation of steam. *Int. J. Heat Mass Transfer* **7,** 272 (1964).
36. E. J. Le Fevre and J. W. Rose, An experimental study of heat transfer by dropwise condensation. *Int. J. Heat Mass Transfer* **8,** 1117 (1965).
37. E. Citakoglu and J. W. Rose, Dropwise condensation—Some factors influencing the validity of heat-transfer measurements. *Int. J. Heat Mass Transfer* **11,** 523 (1968).
38. D. W. Tanner, D. Pope, C. J. Potter, and D. West, Heat transfer in dropwise condensation at low steam pressures in the absence of non-condensable gas. *Int. J. Heat Mass Transfer* **11,** 181 (1968).
39. R. Wilmshurst and J. W. Rose, Dropwise condensation—Further heat-transfer measurements. *Proc. Int. Heat Transfer Conf., 4th* **6,** Cs. 1.4 (1970).
40. T. Tsuruta and H. Tanaka, Microscopic study of dropwise condensation (in Japanese). *Trans. JSME, Ser. B* **49,** 1828 (1983).
41. S. Hatamiya and Tanaka, A study on the mechanism of dropwise condensation (1st Report: Measurement of heat-transfer coefficient of steam at low pressures) (in Japanese). *Trans. JSME, Ser. B* **52,** 1828 (1986).
42. I. Tanasawa, J. Ochiai, Y. Utaka, and S. Enya, Experimental study on dropwise condensation (Effect of departing drop size on heat-transfer coefficients) (in Japanese). *Trans. JSME* **42,** 2846 (1976).
43. H. Tanaka, A theoretical study on dropwise condensation. *J. Heat Transfer* **97,** 72 (1975).
44. H. Tanaka, Measurement of drop-size distribution during transient dropwise condensation. *J. Heat Transfer* **97,** 341 (1975).
45. J. W. Rose, Further aspects of dropwise condensation theory. *Int. J. Heat Mass Transfer* **19,** 1363 (1976).
46. S. Nukiyama, The maximum and minimum value of the heat Q transmitted from metal to boiling water under atmospheric pressure (in Japanese). *J. JSME* **37,** 367 (1934); Engl. transl., *Int. J. Heat Mass Transfer* **9,** 1419 (1966).
47. T. Takeyama and S. Shimizu, On the transition of dropwise-film condensation. *Proc. Int. Heat Transfer Conf., 5th* **3,** 274 (1974).
48. I. Tanasawa and Y. Utaka, Measurement of condensation curves for dropwise condensation of steam at atmospheric pressure. *J. Heat Transfer* **105,** 633 (1983).
49. I. Tanasawa and M. Saito, Film and dropwise condensation of steam on a vertical bank of horizontal circular tubes. *Proc. ASME—JSME Therm. Eng. J. Conf., 2nd, Honolulu* **5,** 143 (1987).
50. B. B. Mikić, On mechanism of dropwise condensation. *Int. J. Heat Mass Transfer* **12,** 1311 (1969).
51. S. N. Aksan and J. W. Rose, Dropwise condensation—The effect of thermal properties of the condenser material. *Int. J. Heat Mass Transfer* **16,** 461 (1973).
52. J. W. Rose, Effect of condenser tube material on heat transfer during dropwise condensation of steam. *Int. J. Heat Mass Transfer* **21,** 835 (1978).
53. S. A. Stylianou and J. W. Rose, Dropwise condensation on surfaces having different thermal conductivities. *J. Heat Transfer* **102,** 477 (1980).
54. D. W. Tanner, C. J. Potter, D. Pope, and D. West, Heat transfer in dropwise condensation—Part II, Surface chemistry. *Int. J. Heat Mass Transfer* **8,** 427 (1965).

55. D. G. Wilkins and L. A. Bromley, Dropwise condensation phenomena. *AIChE J.* **19,** 839 (1973).
56. R. J. Hannemann and B. B. Mikić, An experimental investigation into the effect of surface thermal conductivity on the rate of heat transfer in dropwise condensation. *Int. J. Heat Mass Transfer* **19,** 1309 (1976).
57. T. Tsuruta and H. Tanaka, A theoretical study on constriction resistance in dropwise condensation (in Japanese). *Trans. JSME, Ser. B* **54,** 2811 (1988).
58. T. Tsuruta and S. Togashi, A study on the constriction resistance in dropwise condensation (in Japanese). *Trans. JSME, Ser. B* **55,** 2852 (1989).
59. T. Tsuruta, A study on the constriction resistance in dropwise condensation (in Japanese). Ph.D. Thesis, University of Tokyo, Tokyo, 1989.
60. I. Tanasawa and Y. Shibata, Dropwise condensation at low heat flux and small surface subcooling. *Condens. Heat Transfer, Nat. Heat Transfer Conf., 18th, San Diego,* 79 (1979).
61. K. Kaino, M. Izumi, S. Shimizu, and T. Takeyama, Heat transfer near the initiation of dropwise condensation (in Japanese). *Trans. JSME, Ser. B* **48,** 1339 (1982).
62. I. Tanasawa and S. Nagata, Dropwise condensation heat transfer of steam under small surface subcooling. *Proc. Int. Heat Transfer Conf., 8th* **4,** 1665 (1986).
63. J. W. Rose, Dropwise condensation of mercury. *Int. J. Heat Mass Transfer* **15,** 1431 (1972).
64. M. Kollera and U. Grigull, Über das Abspringen von Tropfen bei der Kondensation von Quecksilver. *Wärme-Stoffüebertrag.* **2,** 31 (1969).
65. M. Kollera and U. Grigull, Untersuchung der Kondensation von Quecksilverdampf. *Wärme-Stoffüebertrag.* **4,** 244 (1971).
66. M. N. Ivanovskii, V. I. Subbotin, and Y. V. Milovanov, Heat transfer with dropwise condensation of mercury vapor. *Teploenergetika* **14,** 81 (1967).
67. E. J. Le Fevre and J. W. Rose, A theory of heat-transfer by dropwise condensation. *Proc. Int. Heat Transfer Conf., 3rd* **2,** 362 (1966).
68. J. W. Rose, On the mechanism of dropwise condensation. *Int. J. Heat Mass Transfer* **10,** 755 (1967).
69. H. Tanaka, A theoretical study on dropwise condensation (in Japanese). *Trans. JSME* **39,** 3099 (1973).
70. H. Tanaka, A theoretical study on dropwise condensation (2nd Report: A theory that excludes overlap between drops) (in Japanese). *Trans. JSME* **40,** 2283 (1974).
71. H. Tanaka, A theoretical study on dropwise condensation. *J. Heat Transfer* **97,** 72 (1975).
72. S. A. Stylianou and J. W. Rose, Dropwise condensation of ethanediol. *Int. J. Phys.-Chem. Hydrodyn.* **3,** 199 (1982).
73. J. Niknijad and J. W. Rose, Dropwise condensation of mercury. *Proc. Int. Heat Transfer Conf., 6th* **2,** 483 (1978).
74. J. Niknijad and J. W. Rose, Comparison between experiment and theory for dropwise condensation of mercury. *Int. J. Heat Mass Transfer* **27,** 2253 (1984).
75. I. Tanasawa and J. Ochiai, Experimental study on dropwise condensation (in Japanese). *Trans. JSME* **38,** 3193 (1972); Engl. transl., *Bull. JSME* **16,** 1184 (1973).
76. L. R. Glicksman and A. W. Hunt, Jr., Numerical simulation of dropwise condensation. *Int. J. Heat Mass Transfer* **15,** 2251 (1972).
77. J. W. Rose and L. R. Glicksman, Dropwise condensation—the distribution of drop sizes. *Int. J. Heat Mass Transfer* **16,** 411 (1973).
78. N. Fatika and D. L. Katz, Dropwise condensation. *Chem. Eng. Prog.* **45,** 661 (1949).
79. L. C. F. Blackman, M. J. S. Dewar, and H. Hampson, An investigation of compounds promoting the dropwise condensation of steam. *J. Appl. Chem.* **7,** 160 (1957).
80. R. A. Erb and E. Thelen, Dropwise condensation characteristics of permanent hydrophobic systems. *U.S. Off. Saline Water Res. Dev. Rep.* No. 184 (1966).

81. D. G. Wilkins, L. A. Bromley, and S. M. Read, Dropwise and filmwise condensation of water vapor on gold. *AIChE J.* **19,** 119 (1973).
82. R. A. Erb, Dropwise condensation on gold. *Gold Bull.* **6,** 2 (1973).
83. D. W. Woodruff and J. W. Westwater, Steam condensation on electroplated gold: Effect of plating thickness. *Int. J. Heat Mass Transfer* **22,** 629 (1979).
84. C. A. Nash and J. W. Westwater, A study of novel surfaces for dropwise condensation. *Proc. ASME–JSME Therm. Eng. J. Conf., 2nd* **2,** 485 (1987).
85. W. M. Rohsenow and H. Y. Choi, "Heat, Mass and Momentum Transfer." Prentice-Hall, Englewood Cliffs, New Jersey, 1961.
86. T. Fujii and H. Uehara, Film condensation heat transfer (in Japanese). *In* "Progress in Heat Transfer," Vol. 1, p. 1. Yokendo Book Co., Tokyo, 1973.
87. J. W. Rose, Fundamentals of condensation heat transfer: Laminar film condensation. *JSME Int. J., Ser. 2* **31,** 357 (1988).
88. J. W. Rose, Condensation heat transfer theory. *Int. Commun. Heat Mass Transfer* **15,** 449 (1988).
89. T. Fujii and H. Honda, Forced convection condensation on a horizontal tube (1st Report: Theoretical treatment) (in Japanese). *Trans. JSME, Ser. B* **46,** 95 (1980).
90. T. Fujii, H. Honda, and K. Oda, Forced convection condensation on a horizontal tube (2nd Report: Experiments for horizontal flow of low-pressure steam) (in Japanese). *Trans. JSME, Ser. B* **46,** 103 (1980).
91. H. Honda and T. Fujii, Effect of wall conduction upon forced convection condensation on a horizontal tube (in Japanese). *Trans. JSME, Ser. B* **46,** 2420 (1980).
92. T. Fujii, H. Honda, K. Oda, Y. Kato, and S. Kawano, Film condensation of fluoro-carbon refrigerant vapors flowing across a horizontal tube (in Japanese). *Trans. JSME, Ser. B* **47,** 197 (1981).
93. I. I. Gogonin and A. R. Dorokhov, Experimental investigation of heat transfer with condensation of moving vapor of R-21 on horizontal cylinders. *J. Appl Mech. Tech. Phys.* **17,** 252 (1976).
94. W. J. Minkowycz and E. M. Sparrow, Condensation heat transfer in the presence of noncondensables, interfacial resistance, superheating, variable properties and diffusion. *Int. J. Heat Mass Transfer* **9,** 1125 (1966).
95. J. W. Rose, Condensation of a vapour in the presence of a non-condensing gas. *Int. J. Heat* Mass Transfer **12,** 233 (1969).
96. L. Slegers and R. A. Seban, Laminar film condensation of steam containing small concentrations of air. *Int. J. Heat Mass Transfer* **13,** 1941 (1970).
97. Y. Mori and K. Hijikata, Free convective condensation heat transfer with noncondensable gas on a vertical surface. *Int. J. Heat Mass Transfer* **16,** 2229 (1973); also *Trans. JSME, Ser. B* **38,** 418 (1972).
98. T. Fujii and Y. Kato, Laminar film condensation of a binary miscible vapour on a flat plate (in Japanese). *Trans. JSME, Ser. B* **46,** 306 (1980).
99. K. Hijikata, Y. Mori, and K. Utsunomiya, Nonsimilar solution of condensation heat transfer containing noncondensable gas (in Japanese). *Trans. JSME, Ser. B* **46,** 1514 (1980).
100. M. Goto and T. Fujii, Film condensation of binary refrigerant vapours on a horizontal tube. *Proc. Int. Heat Transfer Conf., 7th* **5,** 71 (1982).
101. R. Gregorig, Film condensation on finely rippled surfaces with consideration of surface tension. *Z. Angew. Math. Phys.* **5,** 36 (1954).
102. S. Hirasawa, K. Hijikata, Y. Mori, and W. Nakayama, Effect of surface tension on film condensation (A study on the liquid film in small grooves) (in Japanese). *Trans. JSME, Ser. B* **44,** 2041 (1978).

103. S. Hirasawa, K. Hijikata, Y. Mori, and W. Nakayama, Effect of surface tension on laminar film condensation along a vertical plate with a small leading radius. *Proc. Int. Heat Transfer Conf., 6th* **2,** 413 (1978).
104. S. Hirasawa, Y. Mori, K. Hijikata, and W. Nakayama, Optimum surface geometry of vertical condenser tubes (Effect of thermal conduction in fins) (in Japanese). *Trans. JSME, Ser. B* **48,** 527 (1982).
105. Y. Mori, K. Hijikata, S. Hirasawa, and W. Nakayama, Optimized performance of condensers with outside condensing surface. *J. Heat Transfer* **103,** 96 (1981).
106. H. Honda, S. Nozu, and K. Mitsumori, Augmentation of condensation on horizontal finned tubes by attaching a porous drainage plate (in Japanese). *Trans. JSME, Ser. B* **49,** 1937 (1983); Engl. transl., *Proc. ASME–JSME Therm. Eng. J. Conf., 1st, Honolulu* **3,** 289 (1983).
107. H. Honda and S. Nozu, Augmentation of condensation on horizontal finned tubes by attaching a drainage strip (Effect of material and height of the drainage strip). *Trans. JSME, Ser. B* **51,** 3191 (1985).
108. T. M. Rudy and R. L. Webb, An analytical model to predict condensate retention on horizontal integral-fin tubes. *J. Heat Transfer* **107,** 361 (1981).
109. H. Masuda and J. W. Rose, An experimental study on condensation of refrigerant 113 on low integral-fin tubes. *In* "Heat Transfer Science and Technology" (B. X. Wang, ed.), p. 480. Hemisphere, New York, 1987.
110. H. Honda and S. Nozu, A prediction method for heat transfer during film condensation on horizontal low integral-fin tubes. *Trans. JSME, Ser. B* **51,** 572 (1985); Engl. transl., *J. Heat Transfer* **109,** 218 (1987).
111. H. Honda, S. Nozu, and B. Uchima, A generalized prediction method for heat transfer during film condensation on horizontal low integral-fin tubes (in Japanese). *Trans. JSME, Ser. B* **53,** 1329 (1987).
112. D. G. Thomas, Enhancement of film condensation rates on vertical tubes by vertical wires. *Ind. Eng. Chem., Fundam.* **6,** 97 (1967).
113. T. Fujii, W. C. Wang, S. Koyama, and Y. Shimizu, Heat transfer enhancement for gravity controlled condensation on a horizontal tube by a coiled wire (in Japanese). *Trans. JSME, Ser. B* **51,** 2436 (1985).
114. L. R. Glicksman, B. B. Mikić, and D. F. Snow, Augmentation of film condensation on the outside of horizontal tubes. *AIChE J.* **19,** 636 (1973).
115. S. Kumagai, A. Yamauchi, H. Fukushima, and T. Takeyama, Condensation heat transfer on various dropwise-filmwise coexisting surfaces. *Proc. ASME–JSME Therm. Eng. J. Conf., 2nd, Honolulu* **4,** 409 (1987).
116. S. Kumagai, S. Tanaka, H. Katsuda, and R. Shimada, On the effect of co-existence of dropwise condensation to filmwise condensation heat transfer. *Proc. Int. Symp. Condensers Condens., 2nd, Bath, Engl.* p. 483 (1990).
117. A. E. Bergles, Enhancement of heat transfer. *Proc. Int. Heat Transfer Conf., 6th* **6,** 89 (1978).
118. R. L. Webb, Special surface geometries for heat transfer augmentation. *In* "Developments in Heat Exchanger Technology—1" (D. Chisholm, ed.), p. 179. Appl. Sci., London, 1980.
119. R. L. Webb, Enhancement of film condensation. *Int. Commun. Heat Mass Transfer* **15,** 475 (1988).
120. P. J. Marto, Recent progress in enhancing film condensation heat transfer on horizontal tubes. *Proc. Int. Heat Transfer Conf., 8th* **1,** 161 (1986).
121. J. A. Stratton, "Electromagnetic Theory." McGraw-Hill, New York, 1941.
122. T. B. Jones, Electrohydrodynamically enhanced heat transfer in liquids—A review. *Adv. Heat Transfer* **14,** 107 (1978).
123. K. Takano, I. Tanasawa, and S. Nishio, Enhancement of evaporation of a droplet from a hot surface by electric field. *Int. Heat Transfer Conf., 9th, Jerusalem,* **4,** (1990).
124. H. Y. Choi, Electrohydrodynamic condensation heat transfer. *J. Heat Transfer* **90,** 98 (1968).

125. A. Yabe, K. Kikuchi, T. Taketani, T. Yamanishi, Y. Mori, and K. Hijikata, Augmentation of condensation heat transfer by applying non-uniform electric field (in Japanese). *Trans. JSME, Ser. B* **48,** 2271 (1982).
126. T. Taketani, A. Yabe, K. Kikuchi, Y. Mori, and K. Hijikata, Augmentation of condensation heat transfer by applying non-uniform electric field (2nd Report: Augmentation of condensation outside a vertical tube by use of helical wire electrodes) (in Japanese). *Trans. JSME, Ser. B* **52,** 2202 (1986).
127. A. Yabe, T. Taketani, K. Kikuchi, Y. Mori, and H. Maki, Augmentation of condensation heat transfer by applying electro-hydro-dynamical pseudo-dropwise condensation. *Proc. Int. Heat Transfer Conf., 8th* **6,** 2957 (1986).
128. O. J. Foust, ed., "Sodium–NaK Engineering Handbook," Vol. 1. Gordon & Breach, New York, 1972.
129. "JSME Data Book: Heat Transfer," 3rd Ed. Jpn. Soc. Mech. Eng., Tokyo, 1975.
130. "JSME Data Book: Heat Transfer," 4th Ed. Jpn Soc. Mech. Eng., Tokyo, 1986.
131. "1980 SI JSME Steam Tables." Jpn. Soc. Mech. Eng., Tokyo, 1981.
132. "Mechanical Engineering Handbook. A6: Thermal Engineering," New Ed. Jpn. Soc. Mech. Eng., Tokyo, 1985.